RADIO FREQUENCY PROPAGATION DIFFERENCES THROUGH VARIOUS TRANSMISSIVE MATERIALS

Patrick L. Ryan, B.S.I.E.

Thesis Prepared for the Degree of

MASTER OF SCIENCE

UNIVERSITY OF NORTH TEXAS

December 2002

APPROVED:

Perry R. McNeill, Major Professor
Richard White, Co-Major Professor
David Shelton, AT&T Wireless Services, Industry Representative
Michael R. Kozak, Committee Member
Roman Stemprok, Committee Member
Fredrik Williams, Committee Member
Robert L. Getty, Committee Member
Albert B. Grubbs, Jr., Chair of the Department of Engineering Technology
C. Neal Tate, Dean of the Robert B. Toulouse School of Graduate Studies

Ryan, Patrick L., Radio frequency propagation differences through various transmissive materials. Master of Science (Engineering Technology), December 2002, 87 pp., 7 tables, 12 illustrations, references, 47 titles.

The purpose of this research was to determine which of the commonly used wireless telecommunication site concealment materials has the least effect on signal potency. The tested materials were Tuff Span® fiberglass panels manufactured by Enduro Composite Systems, Lexan® XL-1 polycarbonate plastic manufactured by GE Corporation and Styrofoam™ polystyrene board manufactured by The Dow Chemical Company. Testing was conducted in a double electrically isolated copper mesh screen room at the University of North Texas Engineering Technology Building in Denton, Texas. Analysis of the data found no differences exist between the radio frequency transmissiveness of these products at broadband personal communication service frequencies. However, differences in the signal do exist with regards to the angle of incidence between the material and the transmitting antenna.

ACKNOWLEDGMENTS

I express my gratitude to my advisor and major professor Dr. Perry R. McNeill. His attention to detail, encouragement, and guidance have been necessary for this thesis.

I thank my graduate coordinator Dr. Michael R. Kozak for his confidence, encouragement and guidance throughout my graduate program and in writing this thesis.

I thank the Engineering Technology Department, University of North Texas and specifically, Dr. Albert B. Grubbs, for supplying the specialized equipment and screen room for this project. I appreciate the availability of such state-of-the-art facilities and staff assistance for this research project.

I thank David Shelton of AT&T Wireless for his curiosity, knowledge, guidance and support on this project.

I express my gratitude to my committee members Dr. Richard White, Dr. Roman Stemprok, Dr. Fredrik Williams and Dr. Robert L. Getty for their guidance.

I thank Mr. Richard Locke, Enduro Systems, Inc. of Fort Worth, Texas, for donating the Tuff Span sheet stock for this study.

I thank Richard Rodriguez, Director of SpectraSite Construction, Inc., San Antonio, Texas, for donating the antennas and lending his support.

I thank Kerry Senum, who donated the transmission cable and connectors as well as his time, energy, equipment and expertise to complete the verification testing of the installed system.

Thank you, Brian Urban, for your curiosity, support and assistance with equipment and hardware from the Engineering Technology Department.

TABLE OF CONTENTS

LIST OF TABLES

LIST OF ILLUSTRATIONS

Figure Page

CHAPTER 1

INTRODUCTION

The growth and popularity of mobile communication requires the installation of transmission towers in diverse locations. Wireless service providers are increasingly required to camouflage or screen tower placements to hide them from public view. In fact, many municipalities require the use of such "aesthetically pleasing" structures to maintain the beauty of their skylines. Radio frequency (RF) waves are a form of electromagnetic waves used in the communication bandwidths defined by the Federal Communications Commission (FCC) [44]. Companies have emerged in the telecommunication marketplace selling site concealment solutions that use polycarbonate plastic in sheet-stock form like Lexan®, manufactured by GE Corporation; glass reinforced polyester sheet-stock like Tuff Span® fiberglass manufactured by Enduro Composite Systems; and polystyrene foam sheet-stock like Styrofoam™ manufactured by The Dow Chemical Company.

Issues and questions surrounding the subject of RF site concealment will be explored to formulate hypotheses concerning which material has better RF penetration. Answers to questions like, "Which product should be used to affect maximum RF penetration with minimal costs for my site?" will be addressed and answered. Using certain limitations and assumptions, the expectation is to show polystyrene foam as the clear choice for concealment products in personal communication services (PCS) frequency levels.

Purpose of the Study

Known optimization of transmission signals through materials aids in site selection, tuning and maintenance, increasing the efficiency of the network and reducing the overall number of sites required to meet capacity. The purpose of this research is to determine which of the most commonly used site concealment materials (Styrofoam, Lexan and Tuff Span) has the least effect on signal potency.

Statement of the Problem

The problem is optimizing RF propagation at broadband PCS frequencies through polycarbonate plastic in sheet-stock form (Lexan), glass reinforced polyester sheet-stock (Tuff Span) and polystyrene foam sheet-stock (Styrofoam) to provide concealment of tower mounted telecommunication sites.

Significance of the Study

The study should show superior RF propagation through polystyrene over other types of products, affecting the sales and marketing programs of companies that do not deal in polystyrene. RF engineers will have concrete evidence to support their choice of concealment products and will be able to show advantages and disadvantages of competing concealment types. Average base site construction costs, excluding radio equipment, are $175,000. In addition, average concealment costs per site range from $5,000 to $100,000, which is 3% to 57% of the base construction cost for a concealment site. The results of this study may reduce these concealment costs, or at least reduce the range of costs used for budgeting of site construction.

Research Questions

There are two research questions addressed in this study and defined below for hypothesis testing:

1. Question: Which product has the least effect on electromagnetic wave propagation; Lexan, Tuff Span or Styrofoam?

   Null: There is no difference in signal transmission through Styrofoam, Lexan and Tuff Span panels at PCS frequency levels.

   $$H_{o1}: \mu_{T_{st}} = \mu_{T_{lx}} = \mu_{T_{ts}}$$

   Alternative: There is a difference in signal transmission through at least two of the materials at PCS frequency levels.

   $$H_{a1}: \mu_{T_{st}} \neq \mu_{T_{lx}} \neq \mu_{T_{ts}}$$

2. Question: Does the angle of incidence to the material affect the propagation loss difference between materials?

   Null: There is no difference in signal transmission at various angles through Styrofoam, Lexan and Tuff Span panels at PCS frequency levels.

   $$H_{o1}: \mu_{T\Theta_{st}} = \mu_{T\Theta_{lx}} = \mu_{T\Theta_{ts}}$$

   Alternative: There is a difference in signal transmission in at least two of the angles through Styrofoam, Lexan and Tuff Span panels at PCS frequency levels.

   $$H_{a1}: \mu_{T\Theta_{st}} \neq \mu_{T\Theta_{lx}} \neq \mu_{T\Theta_{ts}}$$

Assumptions

Equipment used was within calibration standards and did not stray from calibration during testing. Loads, shorts and other electronic standards used during testing were also within calibration standards. Test results are assumed as consistent, valid, reliable and reproducible. Temperature and the A/C power supply remained constant throughout testing. The screen room filtered out transient RF and electromagnetic waves to an acceptable level. Time of testing was not an issue as tests were performed in a controlled environment. Transmission power levels were held constant during testing. Statistical expert help was provided by Dr. Robert L. Getty and was sought to prove accuracy of the data. Materials used and tested are assumed to be within specifications and standards of the manufacturer and are free from defects.

Limitations

The research performed for this study was limited to the licensed broadband PCS spectrum as defined by the FCC, which covers 1850 – 1990 MHz. Literature review was confined to the libraries of the University of North Texas (electronic resources included), the libraries of the University of Texas at Dallas and the Internet as of May 15, 2002. Facilities and test equipment were limited to those available within budget and within the Dallas-Fort Worth Metroplex. Tests were conducted in a screen room. National Instrument's LabVIEW® software was used to gather test information [32].

CHAPTER 2

REVIEW OF LITERATURE

Supported by a thorough review of literature, different types of wireless communication systems are regulated by the Federal Communications Commission (FCC) and used in our everyday lives. Cellular and personal communication services (PCS) are the two most popular types of services. Providers (or operators) require tower and rooftop sites to affect market penetration of their systems and offer service to over 30 million mobile and portable telephone subscribers in the United States [11][46]. The number of sites required for each type of service is based upon the type of transmission platform used, e.g. code division multiple access (CDMA), time division multiplexing access (TDMA) or global system for mobile communications (GSM) and the number of users in a particular region [29]. Generally, low powered transmitters are inherent to PCS systems, which lose radiated power when loaded. As more users are added to a system, the power radiated from the cell site is reduced and more sites are required to fill in the gaps caused by subscriber growth [29][45].

The increase in base station construction of both tower and rooftop sites has increased public awareness of wireless sites. Communities are concerned about radio frequency (RF) emission safety and the visual affects of telecommunication sites and antennas on their skylines. The FCC published a manual for local and state authorities to clear the myths and misnomers of RF emission safety in June of 2000 [29]. However, skyline aesthetics is still an issue for municipalities [37]. Cities increasingly issue antenna moratoriums and require the use of concealed or “stealth” sites, camouflaged to match the surroundings [46].

Wireless carriers must use creative ways to conceal sites and not degrade the potency of their RF signals. The most popular site concealment types involve using glass reinforced polyester sheet-stock, polycarbonate plastic in sheet-stock form or polystyrene foam sheet-stock painted and formed to look like stucco, brick or other structures that blend into the surrounding environment [31] [34] [40]. The materials chosen for testing in this study are Lexan®, manufactured by GE Corporation, Tuff Span® fiberglass manufactured by Enduro Composite Systems and Styrofoam™ manufactured by The Dow Chemical Company. The characteristics of interest of these materials pertain to their optical and electrical properties listed in Table 1 [16] [18] [19] [21].

Table 1.
Refractive and dielectric constants for tested materials.

Material Property	Method	Tuff Span	Lexan	Styrofoam
Refractive Index, unitless	ASTM D 542	1.46	1.586	1.54
Dielectric Constant, 1 GHz, unitless	ASTM D 150	4.8	2.96	2.5

Researchers at Ohio State University Electro-Science Laboratory (OSU ESL) have tested similar materials and found that Tuff Span and Lexan degrade the signal 400% more in operating frequencies than Styrofoam panels at PCS frequencies. OSU ESL did not, however, complete any modeling or research on why this phenomenon occurs or test the entire PCS bandwidth. The OSU ESL study will be used as a comparison study for the purposes of this thesis. The results of the OSU ESL study should be confirmed through this study [33].

Electromagnetic Wave Propagation

Wireless communication systems use free-space propagation of electromagnetic waves to affect transmission of their respective systems. Free-space propagation for the purpose of this study is propagation through Earth's atmosphere, not through a vacuum. The difference is in signal loss through the Earth's atmosphere, which is not encountered in a vacuum. Basic transmission loss, or path loss, is the signal attenuation between a transmitter and receiver due to separation and multi-path (scattering). Basic transmission loss determines the range of a wireless link. Basic transmission loss is illustrated in Figure 1 [7] with a corresponding loss formula shown in Equation 1.

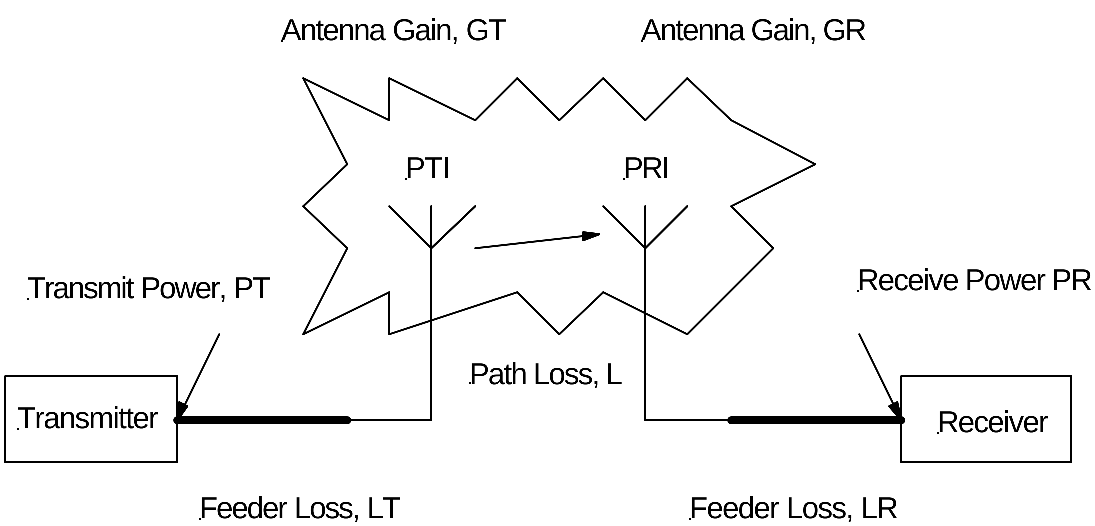

Fig. 1. System path loss.

The path loss, L, can be found through the following relationship:

$$L = PT + GT + GR - PR - LT - LR \qquad (1)$$

Where L = path loss (dBm)

PT = transmit power (dBm)

PTI = transmit power interface

PR = receive power (dBm)

PRI = receive power interface

GT = transmit antenna gain (dBm)

GR = receive antenna gain (dBm)

LT = transmit feeder or transmission cable loss (dBm)

LR = receive feeder or transmission cable loss (dBm)

The free space path loss or atmospheric path loss is given by the following equation:

$$L_a = -32.45 + 20 * \log(\text{freq}) + 20 * \log(\text{dist}) \qquad (2)$$

Where L_a = atmospheric path loss (dBm)

freq = frequency (MHz)

dist = distance (km) [7].

The path loss for the system configuration of this study gives an averages path loss of 19.463 dBm. The calculations used to determine the atmospheric path loss are shown in Appendix E.

To propagate radio waves through Earth's atmosphere, the energy must be radiated from the source (antenna), and captured at the receiver end (another antenna.) Figure 2 shows a point source, several rays propagating from it, and the corresponding wavefront. Although not a perfect source, an omni-directional antenna is a good example of a point source [10].

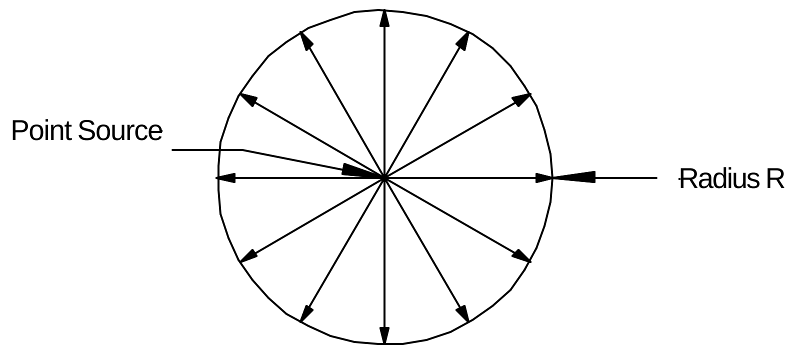

Fig. 2. Wavefront from a point source.

Power density is the rate at which energy passes through a surface area in free space. Field intensity is the magnitude of electric and magnetic fields of an electromagnetic wave propagating in free space [42]. Power density and field intensity are related according to Equation 3 shown below:

$$P = E * H \quad \text{W/m2} \tag{3}$$

Where P = power density (watts per meter squared)

E = rms electric field intensity (volts per meter)

H = rms magnetic field intensity (ampere-turns per meter)

The electric and magnetic field intensities of an electromagnetic wave in free space are related through the characteristic impedance (resistance) of free space, which is 377 ohms [8] [42]:

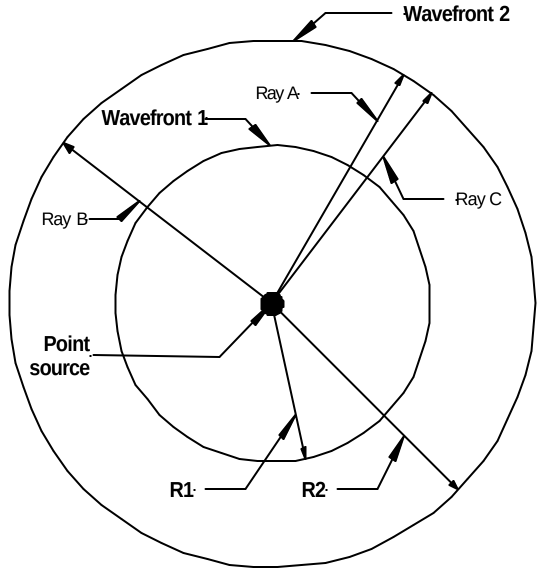

Fig. 3. Spherical wavefront from a point source.

Mathematically, the power density at any point on a spherical wavefront is:

$$P_a = \frac{P_{rad}}{4pR^2} \quad (4)$$

Where P_{rad} = total power radiated (watts)

R = radius of the sphere (which is equal to the distance from any point on the surface of the sphere to the source)

$4pR^2$ = area of the sphere

The power density relationship shown above means the farther the wavefront moves from the source, the smaller the power density. The total power distributed over the surface of the sphere remains the same. However, because the area of the sphere increases in direct proportion to the distance from the source squared, the power density is inversely proportional to the square of the distance from the source [42]. The ratio of the power densities from wavefront 1 and wavefront 2 gives the following refined equation:

$$\frac{P_1}{P_2} = \left(\frac{R_1}{R_2}\right)^2 \qquad (5)$$

The inverse square law of radiation shows that as the distance from the source doubles, the power density decreases by a factor of 2^2 or 4 [10].

Wave Properties of Radio Waves

As waves propagate through free-space they spread out, resulting in a reduction in power density. This reduction is called attenuation. The reduction in power density with distance is equivalent to a power loss and is commonly called wave attenuation. Because the attenuation is due to the spherical spreading of the wave, it is sometimes called the space attenuation of the wave. Wave attenuation is generally expressed in terms of the common logarithm of the power density ratio (dB loss) [41] [42]. The small distances encountered in this study make attenuation negligible. However, wave attenuation (γ_a) is defined as:

$$g_a = 10\log\left(\frac{P_1}{P_2}\right) \qquad (6)$$

The absorption of radio waves by tiny particles like water vapor and dust in the atmosphere is called absorption loss. Absorption of radio frequencies in a normal atmosphere depends on frequency and is relatively insignificant below approximately 10 GHz, not interfering in this study at 1.9 GHz [42].

Optical Properties of Radio Waves

Radio waves also have optical properties, which mean they are subject to refraction, reflection, diffraction and interference as light waves are. Refraction is how waves bend around objects, reflection is how they bounce, diffraction is how they scatter and interference is collision. All of these phenomena can be explained through the use of Maxwell's equations and geometric ray tracing [27] [41].

Refraction through materials is governed by Snell's law, which includes the angle of incidence (Θ_1), angle of reflection (Θ_3), angle of refraction (Θ_2) and the refractive indexes of the two materials being met (n_1 and n_2) as seen in Figure 4 [41].

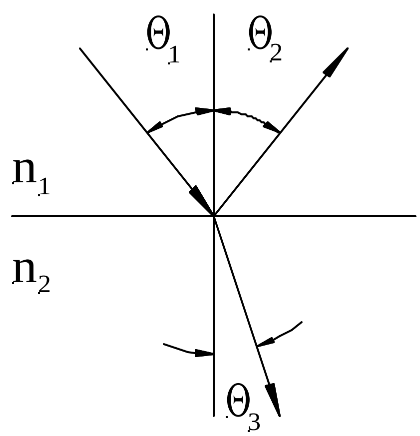

Fig. 4. Snell's Law of reflection and refraction.

The amount of bending or refraction that occurs at the interface of two materials depends on the refractive indexes of the materials:

$$n = \frac{c}{v} \tag{7}$$

Where n = refractive index (unitless)

c = speed of light in free space (3×10^8 m/s)

v = speed of light in a given material (meters per second)

Snell's law uses refractive indexes to show how an electromagnetic wave reacts when it meets the interface of two transmissive materials with different indexes [41]:

$$n_1 \sin \Theta_1 = n_2 \sin \Theta_3 \tag{8}$$

Where n_1 = refractive index of material 1 (unitless)

n_2 = refractive index of material 2 (unitless)

Θ_1 = angle of incidence (degrees)

Θ_2 = angle of reflection = angle of incidence (degrees)

Θ_3 = angle of refraction (degrees)

and since the refractive index of a material is equal to the square root of its dielectric constant:

$$\frac{\sin \Theta_1}{\sin \Theta_3} = \sqrt{\frac{e_{r2}}{e_{r1}}} \tag{9}$$

Where ε_{r1} = dielectric constant of medium 1 (unitless)

ε_{r2} = dielectric constant of medium 2 (unitless)

As waves enter from air into a medium, they are bent towards the normal. When waves leave the medium and re-enter air, the waves are bent back, away from the normal, to their original trajectory. For the purposes of this study, refraction will not be a contributing loss factor as the signal will pass from air to the medium and back to air continuing its original trajectory [41].

The reflection of radio waves occurs when an incident wave strikes a boundary of two media and some or all of the incident power does not enter the second material. The waves that do not penetrate the second medium are reflected. Because all the reflected waves remain in medium 1, the velocities of the reflected and incident waves are equal. Consequently, the angle of reflection equals the angle of incidence [42].

For the purpose of this study, the transmission line approach to compute reflected and transmitted waves will be used [8] [25], which is illustrated below in figure 5.

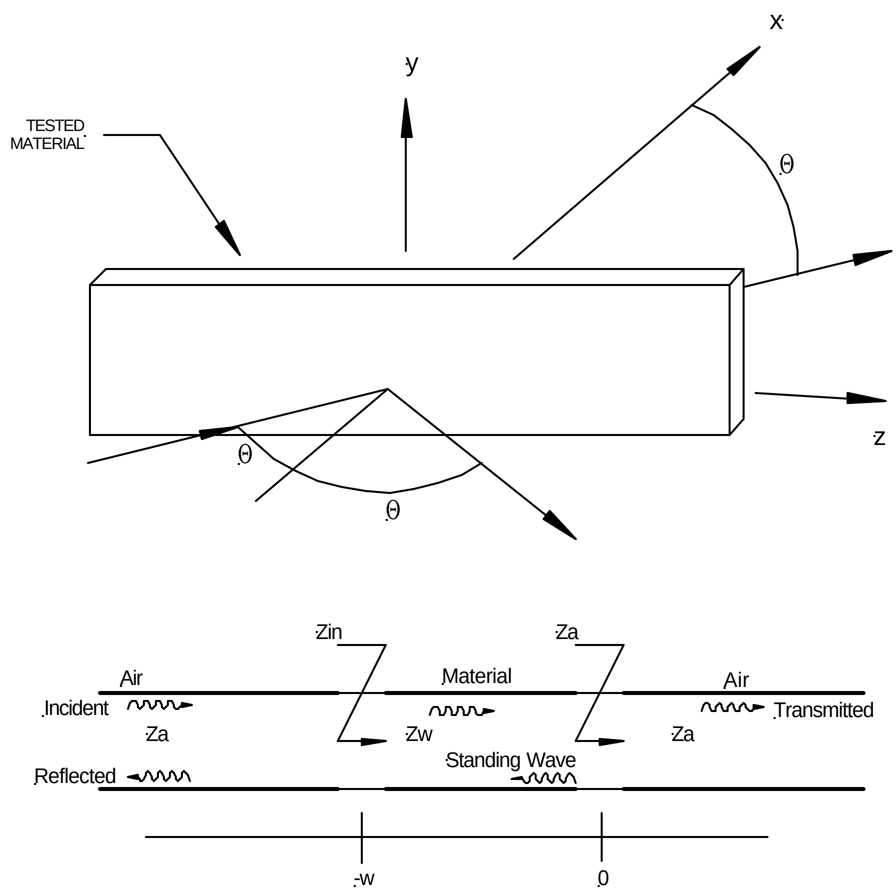

Fig. 5. Transmission line approach to compute reflected and transmitted waves.

The impedance difference between air and the material is characterized by the following relationship [8].

$$Z_{in} = Z_w \left(\frac{Z_L \cos B_w w + jZ_w \sin B_w w}{Z_w \cos B_w w + jZ_L \sin B_w w} \right) \tag{10}$$

Where Z_{in} = input impedance to the dielectric medium (?)

Z_w = impedance of the dielectric medium (?)

Z_L = load impedance, which in this case is Z_a (?)

Z_a = characteristic impedance of air (?)

w = thickness of the dielectric material (meters)

B_w = wavenumber along x of the material (unitless)

and $$B_w = k_w \cos\Theta_w \quad (11)$$

Where Θ_w = the angle of incidence with the dielectric in degrees

and $$k_w = \frac{w}{v} = \left(\frac{w}{c}\right)\sqrt{e_r} \quad (12)$$

for the harmonic time dependence at frequency $f = \omega/2\pi$. The wavelength relationship with the wavenumber, k_w is defined by $\lambda_w = 2\pi/k_w$ [8].

The ratio of the reflected to the incident voltage intensities is called the reflection coefficient, (Γ). For a perfect conductor, $\Gamma = 1$ [42]. The reflection coefficient is a function of the incident and reflected voltage intensities and the incident and reflected phases as:

$$\Gamma = \frac{E_r e^{j\Theta_r}}{E_i e^{j\Theta_i}} = \frac{E_r}{E_i} = e^{j(\Theta_r - \Theta_i)} \quad (13)$$

Where Γ = reflection coefficient (unitless)

E_i = incident voltage intensity (volts)

E_r = reflected voltage intensity (volts)

Θ_i = incident phase (degrees)

Θ_r = reflected phase (degrees)

The reflection coefficient can also be expressed as the following ratio relating the impedance differences between air and the dielectric material [8]:

$$\Gamma = \frac{Z_{in} - Z}{Z_{in} + Z} \qquad (14)$$

Where Z_{in} = input impedance to the dielectric medium

Z = wave impedance for air = 377 Ω.

The transmission coefficient of the electric field is given by T = 1 + Γ. The reflection coefficient is positive for Θ = 0º and approaches -1 at Θ = 90º. In going from a positive to a negative value, Γ passes through zero, meaning no signal is reflected, at Brewster's angle, Θ_B , which can be found from the expression:

$$\Theta_B = \arctan\sqrt{e_r} \qquad (15)$$

Brewster's angle can be used to explain how transmission can actually get better as the angle of incidence increases for certain dielectric materials [8] [41]. The Brewster's angles for the materials in this study were calculated and are shown in Table 2 below:

Table 2.
Brewster's angle for tested materials with dielectric constants restated.

	ε_r	Θ_B
Styrofoam	2.5	57.68847
Lexan	2.96	59.83321
Tuffspan	4.8	65.46636

Diffraction is the modulation or redistribution of energy within a wavefront when it passes near the edge of an opaque object. Diffraction is what allows waves to propagate around corners. As the wavefront passes the object, the waves scatter or diffract around the object, like light spreading around the edge of a door opened in a dark room. Diffraction can be explained using Huygen's principle, which is derived from Maxwell's equations. Huygen's principle says that every point on a given spherical wavefront can be considered a secondary point source of electromagnetic waves from which other secondary waves are radiated outward [41] [42]. However, diffraction will be negligible as testing will be completed through transmissive, not opaque materials and the transmission angles to the edges of the materials will be large. The transmission angles for this project are illustrated in Figure 6. The antennas used for this study have a vertical beamwidth of 36º +/- 5º [12]. For diffraction to be a factor, the transmit antenna would need a vertical beamwidth greater than 150º, so no diffraction will enter this study.

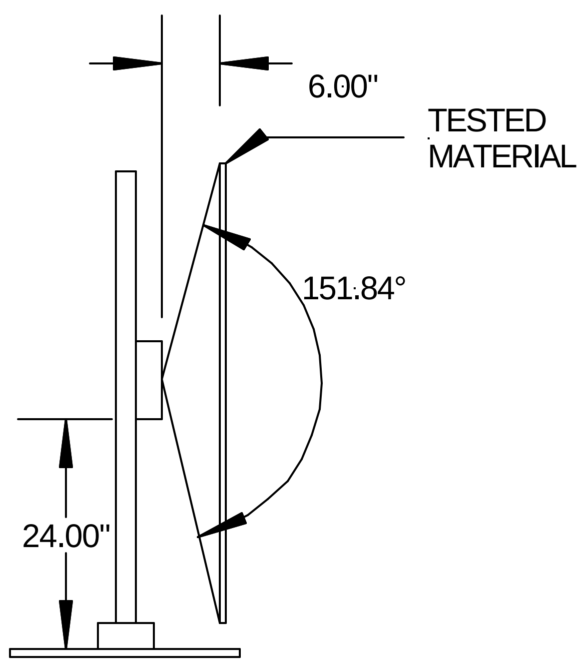

Fig. 6. Diffraction angle of tested materials.

Radio wave interference occurs when two or more electromagnetic waves combine in such a way that system performance is degraded. Since these waves combine, they can be explained through the use of linear superposition theory, which states the total voltage intensity will be the sum of the individual wave vectors. For relatively large wavelengths, which are frequencies below VHF levels or 30 MHz, interference is not a significant problem [42]. However, in the UHF bands interference can be a problem and will be minimized through the use of an indoor screen room and a climate controlled environment [28].

Software

National Instrument's LabVIEW® software was used for this research project [32]. LabVIEW (Laboratory Virtual Instrumentation Engineering Workbench) is a graphical programming language that has been adopted throughout industry, academia and government laboratories as the standard for data acquisition and instrument control software [9]. A LabVIEW program was developed using existing instrument drivers from the National Instrument's Web site and creating additional new instrument drivers for data acquisition and instrument control in this research. The program is included in Appendix A and explained in detail in Chapter 3 of this paper.

CHAPTER 3

METHODOLOGY

The research method employed was experimental. The losses associated with the testing model and the wave and optical characteristics of the signal can be calculated for all of the source materials and angles of incidence given the theories identified in Chapter 2. The calculated losses through the materials are summarized in Table 3:

Table 3.
Calculated losses for materials and angles of incidence.

	90º	60º	30º	0º	-30º	-60º	-90º
Air	-52.6936	-46.0269	-43.4116	-42.6936	-43.4116	-46.0269	-52.6936
Styrofoam	-52.6936	-45.7641	-43.1094	-43.0023	-43.1094	-45.7641	-52.6936
Lexan	-52.6936	-45.9818	-43.359	-42.7476	-43.359	-45.9818	-52.6936
Tuff Span	-52.6936	-45.9257	-43.2945	-42.8131	-43.2945	-45.9257	-52.6936

Lexan® is manufactured by GE Corporation. Tuff Span® fiberglass is manufactured by Enduro Composite Systems. Styrofoam™ is manufactured by The Dow Chemical Company.

The loss differences from the baseline or air are shown in Table 4:

Table 4.
Calculated differences from free space path loss.

	90º	60º	30º	0º	-30º	-60º	-90º
Air	0	0	0	0	0	0	0
Styrofoam	0	0.262856	0.302198	-0.30873	0.302198	0.262856	0
Lexan	0	0.045119	0.052587	-0.05394	0.052587	0.045119	0
Tuff Span	0	0.101239	0.117027	-0.11953	0.117027	0.101239	0

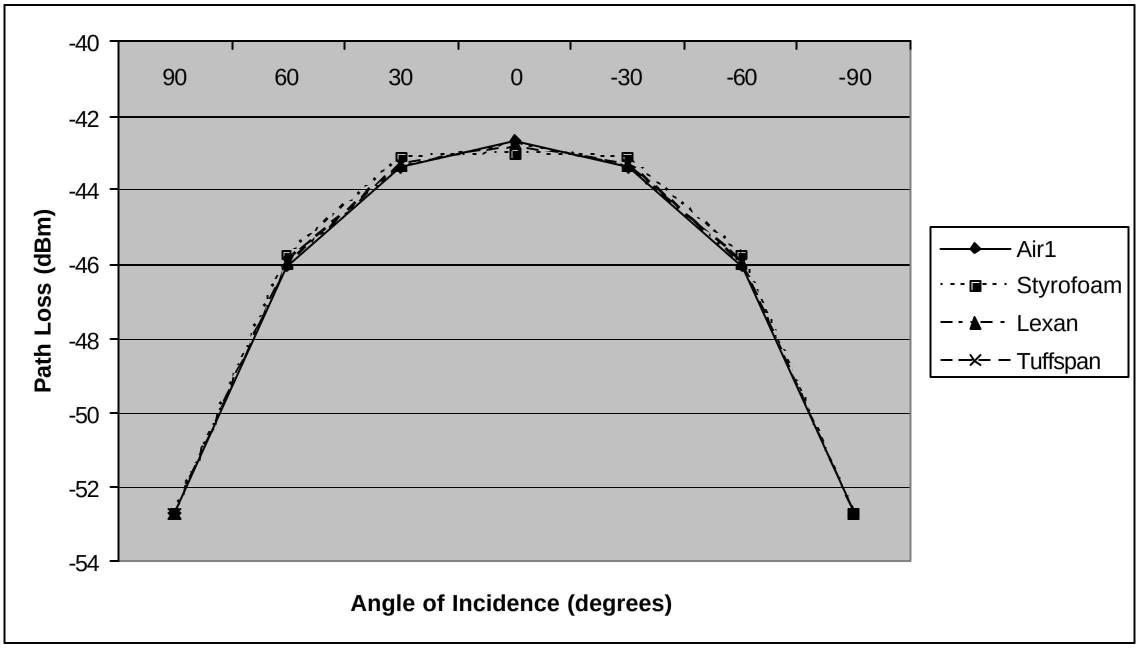

Fig. 7. Calculated path loss values vs. angle of incidence.

Research Design

The data collected pertained to power loss through commonly used materials in tower concealment. A baseline test was conducted to determine the loss through the atmosphere, or free space at the varied source angles as shown in Figure 7. Power transmission levels were set at a constant level of 10 dB for all testing. Testing was completed in an indoor screen room, described below, in a controlled environment so as to minimize transient radio frequency (RF) signals and diminish the effects of time-of-day, temperature, relative humidity and foreign particles. Temperature and relative humidity were recorded and remained constant throughout testing.

Material tests were conducted at the various source angles at 5 MHz intervals through the Federal Communications Commission (FCC) defined broadband personal communication services (PCS) bandwidth of 1850 – 1990 MHz. Statistics was used to explain power loss characteristics over the entire range of the bandwidth. Forty measurements were taken at each frequency level and angle level over five trials, for a total of 162,400 samples. The signal measurements give a complex, sinusoidal waveform. Mean signal strength is taken as the average of these readings over the entire bandwidth. A two-factor Analysis of Variance (ANOVA) table without replication was constructed to test equivalency and variance of angle of incidence and material [14].

Angular testing was completed by changing the transmitting antenna's azimuth, or angle of incidence through seven different stations, then completing the required frequency and trial sampling. Angles were permanently marked on the antenna mount bases. These stations are shown in Figure 8 below:

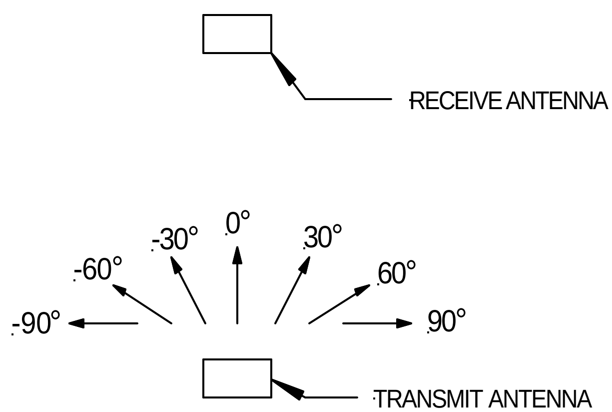

Fig. 8. Angles of incidence tested per trial.

Figure 9 shows the overhead view of the screen room during testing. The distances shown in Figure 9 of 6 inches (0.1524 m) to material and 87 inches (2.2098 m) to receive antenna are due to simulation of the real world site design and size constraints of the screen room. Antennas are placed within 20 inches (0.5 m) of the concealment material when installed on a telecommunication tower [31] [35] [37]. The 87 inch distance from the transmit antenna to the receive antenna was maximized to the constraint of the screen room, which has interior dimensions of 119" (3.0226 m) length by 118" (2.9972 m) width and 97 3/4" (2.4828 m) height. Material and antenna mount locations are marked on the floor to ensure reproducibility of antenna and material location for all testing.

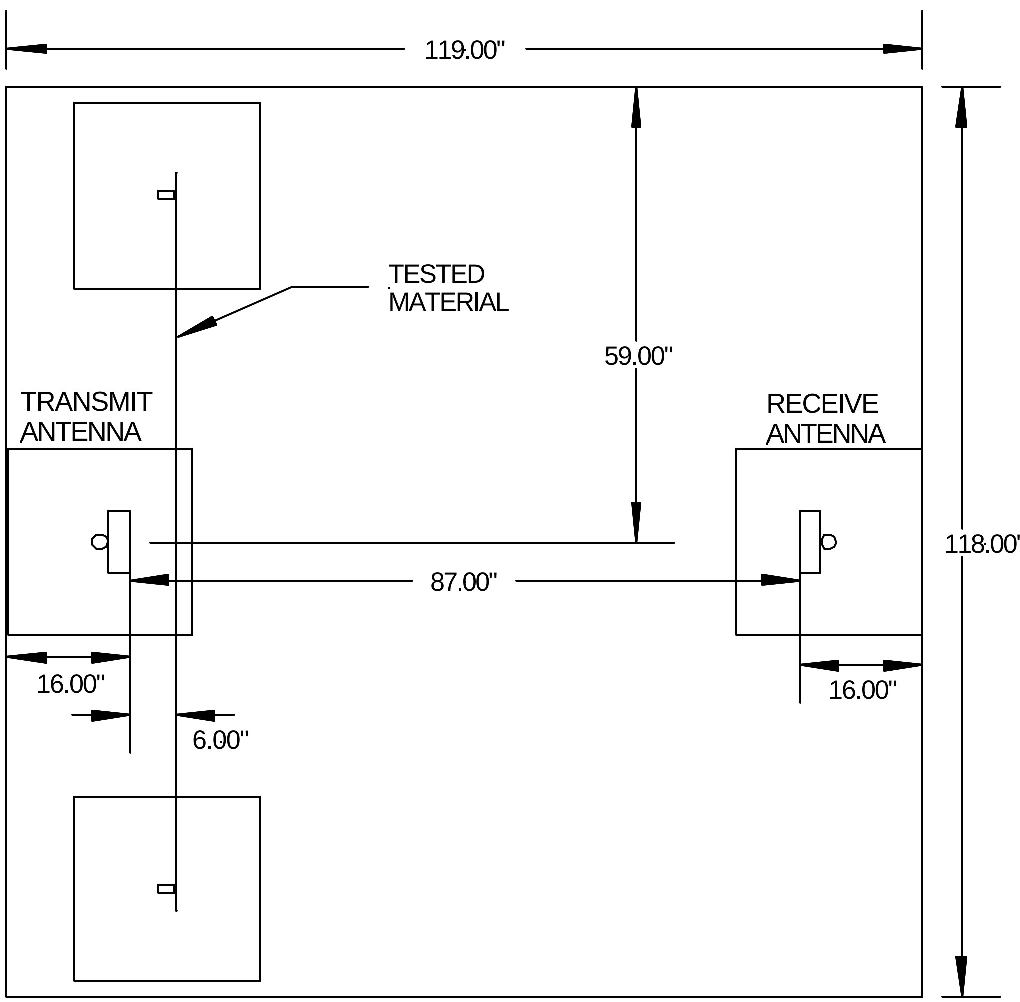

Fig. 9. Overhead view of screen room testing layout.

Figure 10 shows the side view of the screen room dimensioned with the antenna height and material placement during testing. Antenna height was marked on the antenna mount support to ensure reproducibility of height location for all tests. All materials tested were 4’ x 8’ (1.2192 m x 2.4384 m) sheet stock and had mounting holes drilled to the same dimensions to ensure repeatability of material locations during testing.

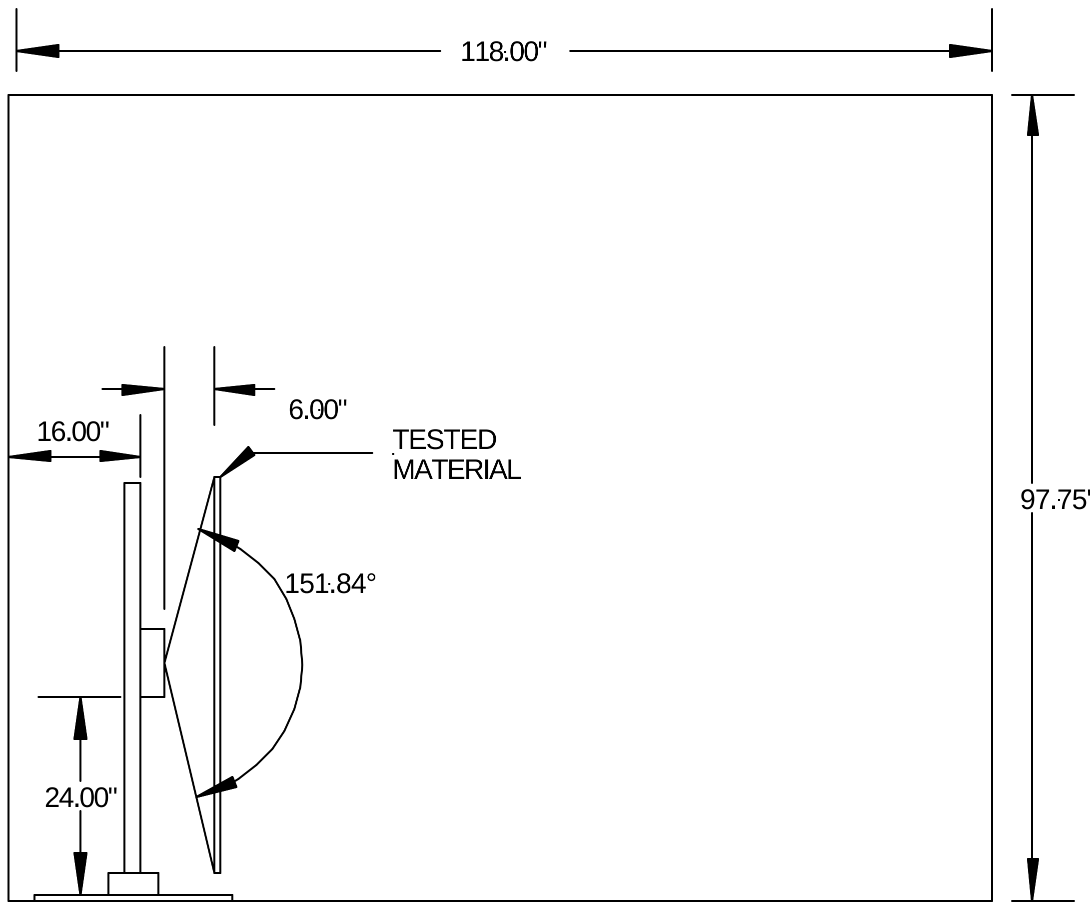

Fig. 10. Side View of Screen Room Testing Layout.

Materials

The tested materials were Tuff Span® fiberglass panels manufactured by Enduro Composite Systems, standard size 4’ x 8’ x 0.093” (1.2192m x 2.4384m x 0.0024m); Lexan® XL-1 polycarbonate plastic manufactured by GE Corporation , standard size 4’ x 8’ x 0.093” (1.2192m x 2.4384m x 0.0024m); and Styrofoam™ polystyrene board manufactured by The Dow Chemical Company, standard size 4’ x 8’ x 0.75” (1.2192m x 2.4384m x 0.0191m). The materials and thicknesses used simulate real-world applications. The optical and electrical properties of these materials were listed in Table 1 of Chapter 1.

The mounts for the antennas and material support were assembled from PVC materials and fastened using brass screws to plywood bases measuring 2’ x 2’ x 0.75” (0.6096m x 0.6096m x 0.0191m). PVC and wood have low RF penetration rates and are accepted as RF transmissive materials. However, due to durability considerations when subjected to the elements, these materials are not suitable for tower concealment. They are used in this study because they are cheap, readily available, easily assembled and induce minimal interference to the study.

Equipment

The screen room was donated to the University of North Texas and was manufactured by Lindgren RF Enclosures. The copper screen enclosure is patented by Lindgren RF Enclosures using a double electrically isolated (DEI) modular enclosure. The screen room is made of 22ga x 22ga x 0.015” copper mesh that is specified to shield from 90-100 dBm of external signal / noise [28]. The screen room was spot tested after assembly and returned an average shielding loss of 84.05 dBm. The enclosure has interior dimensions of 119" (3.0226 m) length by 118" (2.9972 m) width and 97 3/4" (2.4828 m) height.

The antennas used were DB770TB5NPXS indoor directional PCS antennas manufactured by Decibel Products. The operating frequencies of these antennas are 806 – 2200 MHz [12], which includes the broadband PCS frequencies of 1850-1990 MHz. According to manufacturer's specifications, the antennas have a gain of 6.3 dBd and 8.4 dBi with a horizontal beamwidth of 70º ± 10º and a vertical beamwidth of 36º ± 5º. David Shelton with AT&T Wireless Services states that antenna polarization is not an issue at PCS frequencies, and will thus not be discussed.

The transmission cables used were constructed of FSJ4-50B, ½" Superflex™ foam dielectric, 50 ohm cable manufactured by Andrew Corporation [5]. Connectors used on the cables were type-N male, 16N-50-9-6 (90º) and 11N-50-9-9 connectors manufactured by Huber-Suhner [26]. The cables were assembled according to the manufacturer's specifications and tested using the Site Master™ S331-B cable and antenna analyzer manufactured by Anritsu [6]. The results of the cable testing can be found in Appendix G. The cable assemblies contributed a signal loss of 3.57 dBm upon testing, which is within the manufacturer's specifications.

The transmitted signal was generated using an Agilent 8648C Synthesized Signal Generator supplied by the University of North Texas. The 8648C generates signals from 9 kHz to 3200 MHz and was equipped with an IEEE 488.2 port for external programming [23]. The equipment was within calibration at the time of testing and the calibration certificate can be found in Appendix F.

The signal was received by an Agilent E4402B ESA-E Series Spectrum Analyzer supplied by the University of North Texas. The E4402B receives input from 30 Hz to 3.0 GHz and was equipped with an IEEE 488.2 port for external programming [1] [2] [3]. The equipment was within calibration at the time of testing and the calibration certificate can be found in Appendix F.

LabVIEW® Software

The LabVIEW software used for this research project was a compilation of Instrument Drivers downloaded from the National Instrument's Web site and associated code created specifically for this project [9] [32]. A LabVIEW virtual instrument (VI) is roughly equivalent to a subroutine program. A VI can be standalone, or called by another VI, in which case, it is defined as a subVI. A VI has both a diagram (or program) and a front panel (user interface). SubVIs and instrument drivers were used to create the front panel of Thesis Prop.vi, which is shown in Figure 11 below:

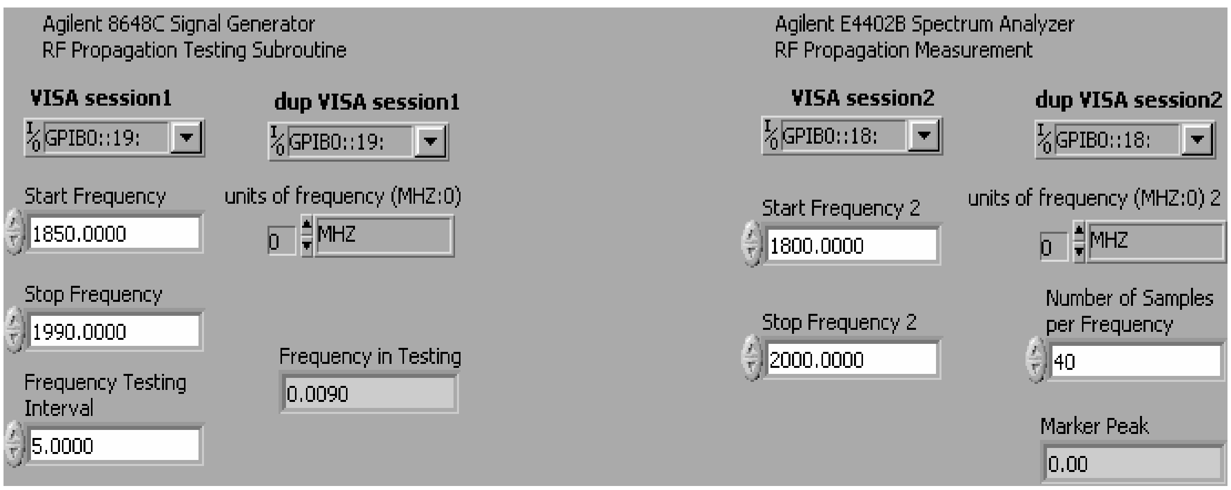

Fig. 11. Front panel of Thesis Prop.vi.

Thesis Prop.vi is the only LabVIEW software program shown in Appendix A and the development of the software was part of this research project. The front panel requires user input to set the Start Frequency, Stop Frequency, Frequency Units, Testing Interval, and GPIB or VISA port identification number for the instrument. These inputs are used to compute the number of iterations the total program must run to complete the testing routine. The signal generation routine waits for the required number of samples to be taken at each frequency from the Spectrum Analyzer portion of the program.

The Signal Generator is controlled by a subVI, called HP8648A Application Function.vi. Although many possible inputs to this application are possible, for this project only the inputs noted in Figure 11 are passed to the application. The remainder of the inputs is left at the default level for the Agilent 8648C.

The Spectrum Analyzer portion of the program requires user input to set the frequency limits for the display through Start Frequency, Stop Frequency, Frequency Units, the number of samples per frequency, and GPIB or VISA port identification number for the instrument. The user inputs are used to initialize the instrument and format the data read during testing. Simultaneously with the initialization of the 8648C, the E4402B Spectrum Analyzer is initialized through the subVI E4402B Configure Frequency.vi.

The Standard Commands for Programmable Instrumentation (SCPI) programming language defines a standard set of commands to control programmable test and measurement devices in instrumentation systems [4]. After initialization, the testing routine is entered where SCPI programming language is used to set the marker peak function of the instrument and query for the results of the peak. These peaks are stored in an array and passed to the last subVI of the program, Write To Spreadsheet File.vi, which prompts the user for a filename. The file naming convention used for this project is illustrated in field notes and sample test logs found in Appendix B.

During testing, Thesis Prop.vi was executed in single-run mode and files saved for each angle of incidence and experiment trial. These files were imported into a spreadsheet program and the data points were refined to statistically significant representations of the data.

CHAPTER 4

ANALYSIS AND RESULTS

The National Instrument's LabVIEW® program shown in Appendix A was used to record samples at each marker peak from the Spectrum Analyzer. Appendix C contains a sample experimental data table. A database was created and contained the following spreadsheets: Master, Air, Styrofoam, Lexan and Tuff Span. Each output data file was moved into its respective material spreadsheet in the database according to material, angle of incidence and test trial. Test iterations were averaged over the entire bandwidth according to the mean signal strength method [43]. Each material was tested for equivalency of means using ANOVA tables and *F*-testing [14]. Table 5 is a summary of all of the test data showing the air baseline and the material results. Individual ANOVA tables for each material tested, showing continuity, are included in Appendix D.

Table 5.
Material test results vs. angle of incidence.

	-90	-60	-30	0	30	60	90
Air	-45.39	-43.76	-41.99	-38.88	-38.73	-44.16	-46.93
Styrofoam	-46.24	-43.85	-41.63	-39.00	-38.75	-44.38	-46.67
Lexan	-44.72	-44.19	-42.80	-38.98	-39.41	-43.04	-46.25
Tuff Span	-44.98	-44.05	-43.23	-40.06	-40.39	-43.19	-46.31

Lexan® is manufactured by GE Corporation. Tuff Span® fiberglass is manufactured by Enduro Composite Systems. Styrofoam™ is manufactured by The Dow Chemical Company.

A graphical representation of the test results are shown in Figure 12.

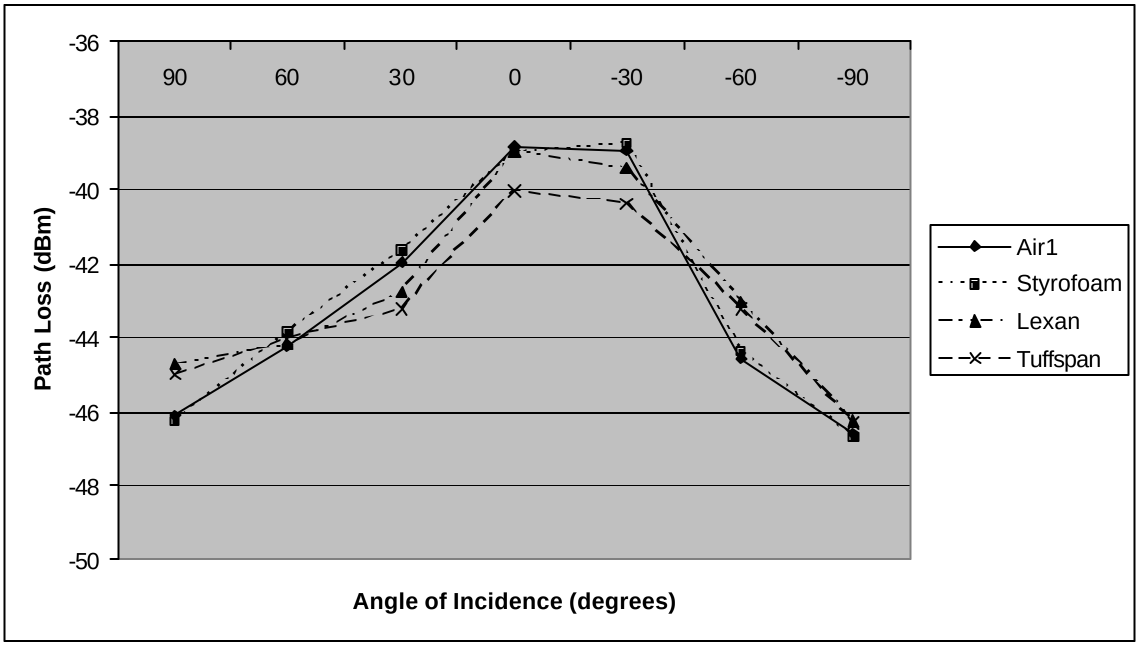

Fig. 12. Tested path loss values vs. angle of incidence.

A two-factor ANOVA table test without replication was completed to test both hypotheses of the study, which is shown in Table 6.

Table 6.
ANOVA table of test results.

ANOVA: Two-Factor Without Replication

SUMMARY	*Count*	*Sum*	*Average*	*Variance*
Air	7	-301.2473	-43.03533	10.27878
Styrofoam	7	-300.5235	-42.93192	10.41784
Lexan	7	-299.3856	-42.76936	7.264663
Tuff Span	7	-302.2207	-43.17438	5.211048
-90	4	-182.0548	-45.5137	0.604063
-60	4	-176.3018	-44.07545	0.028004
-30	4	-169.6223	-42.40558	0.542579
0	4	-156.888	-39.222	0.320548
30	4	-157.4762	-39.36904	0.543796
60	4	-175.206	-43.80151	0.632731
90	4	-185.8278	-46.45695	0.043517

ANOVA

Source of Variation	*SS*	*df*	*MS*	*F*	*p-value*	*F crit*
Material	0.612	3	0.204176	0.487864	0.695002	3.1599
Angle of Incidence	191.5	6	31.9168	76.26287	8.18E-12	2.6613
Error	7.533	18	0.41851			
Total	199.6	27				

Null (H_o) and alternative (H_a) hypothesis comparison for material and angle of incidence are as follows:

1. Table 6 shows through F-test that there is no difference in the means of the tested materials, air included. Therefore, the H_{o1} hypothesis was accepted. There is no difference in signal transmission through Styrofoam, Lexan and Tuff Span panels at personal communication services (PCS) frequency levels.

2. Table 6 shows through F-test that there is a difference in the means of the tested materials through the varied angles of incidence. Therefore, the H_{o2} hypothesis was rejected and the H_{a2} hypothesis was accepted. There is a difference in signal transmission between at least two of the angles through Styrofoam, Lexan and Tuff Span panels at PCS frequency levels.

Tukey's Procedure, also called the T method for identifying significantly different μ_i's, was used to identify the angles of incidence with significant differences [14]. The calculations for Tukey's Procedure can be found in appendix E. The significance groupings are shown in Table 7.

Table 7.
Tukey procedure results for angles of incidence.

Air

0	-30	30	60	-60	90	-90
-38.841	-38.920	-41.968	-44.217	-44.585	-46.114	-46.602

Styrofoam

-30	0	30	60	-60	90	-90
-38.753	-38.998	-41.628	-43.849	-44.385	-46.243	-46.667

Lexan

0	-30	30	-60	60	90	-90
-38.985	-39.410	-42.796	-43.043	-44.185	-44.717	-46.249

Tuffspan

0	-30	-60	30	60	90	-90
-40.065	-40.393	-43.194	-43.230	-44.051	-44.980	-46.309

All materials have means grouped to show differences greater than 1.439 dB, as defined by the studentized Q distribution. Significance groups are underlined to illustrate differences. For air, 0 and -30 degrees are not significantly different from one another, but are significantly higher than 30 degrees. Thrity degrees, in turn, are significantly different from 60 and -60 degrees, which are different from 90 and -90 degrees. The same pattern holds true for Styrofoam and Lexan. However, Tuff Span has only two significance groups, between 0 and -30 degrees and the rest of the angles of incidence. The lack of consistency between 0 and 30 degrees with 0 and -30 degrees may be due to the placement of the materials during testing with the door of the screen room.

CHAPTER 5

CONCLUSIONS AND RECOMMENDATIONS

The purpose of this research was to determine which of the most commonly used site concealment materials has the least effect on signal potency. The tested materials were Tuff Span® fiberglass panels manufactured by Enduro Composite Systems, Lexan® XL-1 polycarbonate plastic manufactured by GE Corporation and Styrofoam™ polystyrene board manufactured by The Dow Chemical Company.

Conclusion

The hypothesis testing results are consistent with the theorized results modeled and calculated in Table 3 of Chapter 3.

Analysis of the data found that statistically, no differences exist between the signal potency of these products at these thicknesses. Therefore, selection of site concealment solutions should depend upon overall cost of the concealment system, not any claim of superior radio frequency (RF) performance. Implementation managers can manage their budgets using minimal cost factors for such concealed sites.

However, differences in the signal transmission do exist with regards to the angle of incidence between the material and the transmitting antenna. When designing concealed communication towers, care should be given to ensure transmission paths are arranged as perpendicular as possible (within 30 degrees according to the Tukey test) to the concealment material.

Recommendations

Further study should be completed for the following cases and situations:

1. The angle of incidence to the vertical plane was tested in this study. Research should be conducted on angle of incidence to the horizontal plane, as well as complex angle combinations between the vertical and horizontal planes.

2. The same testing algorithms can be used to test different angles of reception and distances of reception by keeping the transmit antenna stationary and moving the receive antenna. Such a study would provide insight into multi-path reception characteristics of the system.

3. The effects of different types and placement of material supports should be tested to ascertain their contribution to reflection and path loss.

4. Composite material systems that combine one or more of these products to enhance material stability could be tested in future studies.

APPENDIX A

LabVIEW® SOFTWARE

Thesis Prop.vi

Connector Pane

Front Panel

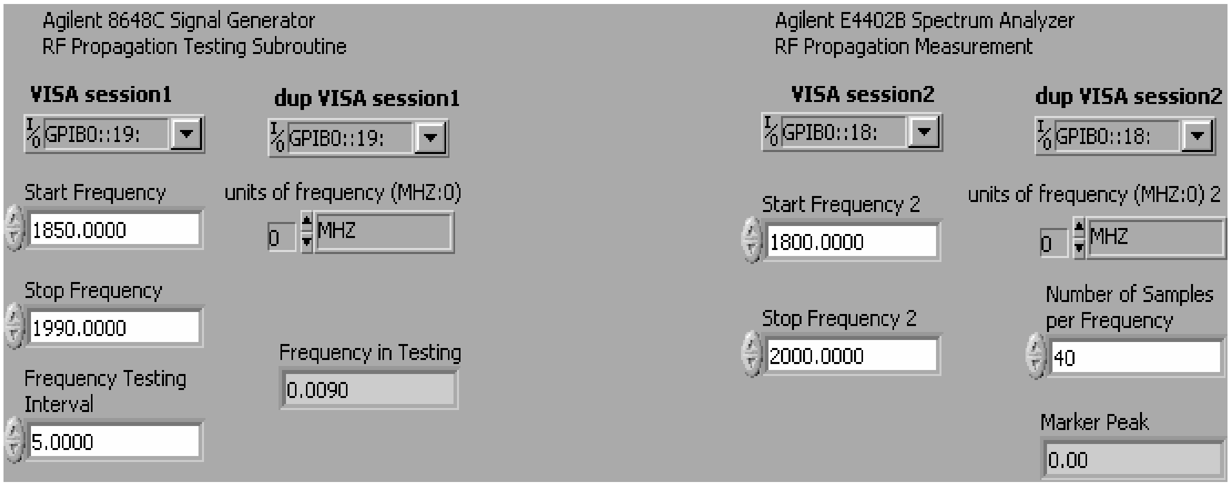

Controls and Indicators

DBL **Start Frequency**

DBL **Stop Frequency**

DBL **Frequency Testing Interval**

I32 **Number of Samples per Frequency**

U16 **units of frequency (MHZ:0)** Sets the units of frequency. Units may be:

0 - MHZ, megahertz
1 - KHZ, kilohertz
2 - HZ, hertz

I/O **VISA session2**

I/O **VISA session1**

DBL **Start Frequency 2**

DBL **Stop Frequency 2**

U16 **units of frequency (MHZ:0) 2** Sets the units of frequency. Units may be:

0 - MHZ, megahertz
1 - KHZ, kilohertz
2 - HZ, hertz

DBL **Frequency in Testing**

I/O **dup VISA session2**

I/O **dup VISA session1**

DBL **Marker Peak**

Block Diagram

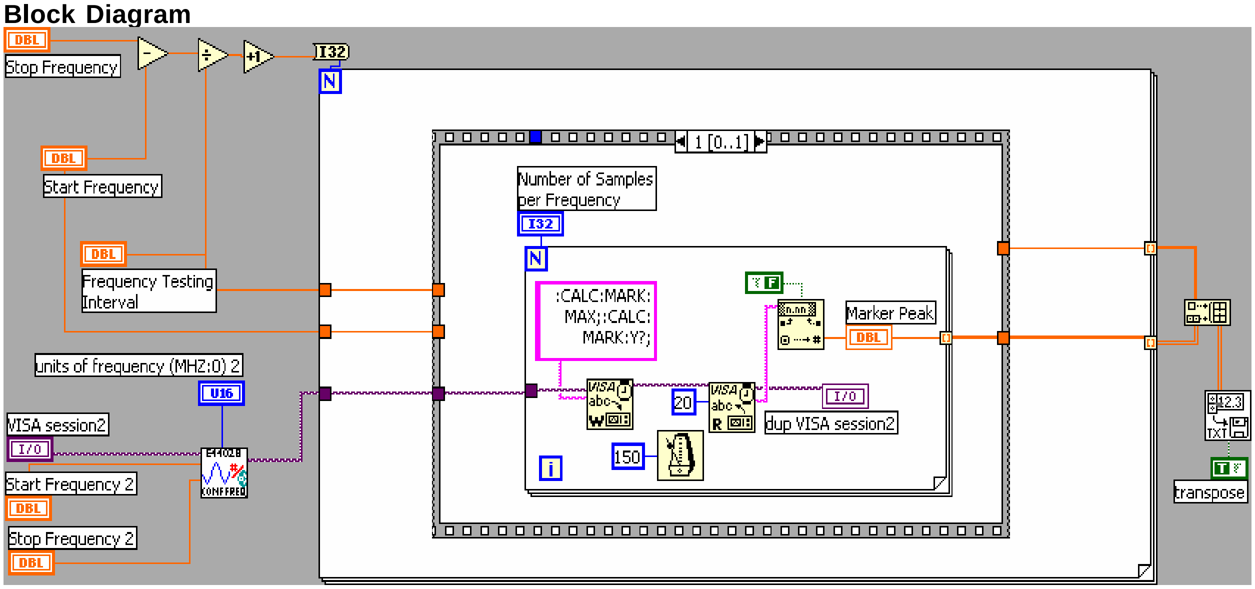

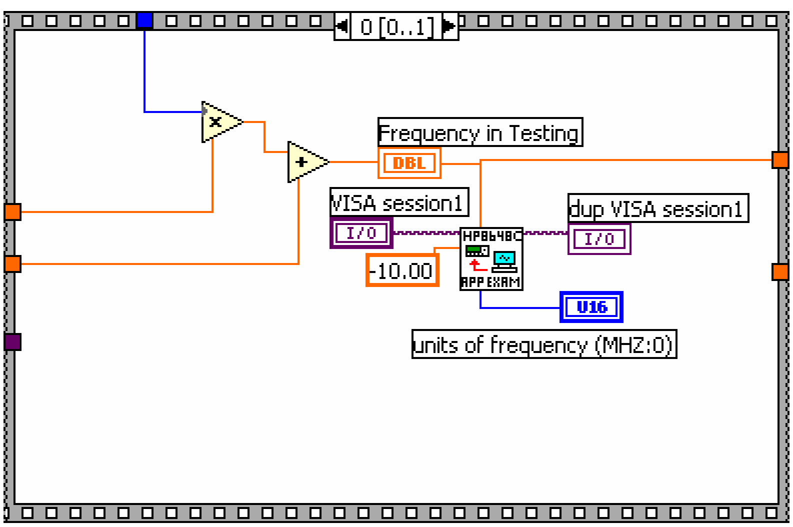

List of SubVIs

HP8648A Application Function.vi
C:\Program Files\National Instruments\LabVIEW 6 SE\instr.lib\hp8648a\hp8648a.llb\HP8648A Application Function.vi

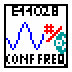

E4402B Configure Frequency.vi
C:\Program Files\National Instruments\LabVIEW 6 SE\instr.lib\E4402B Configure Frequency.vi

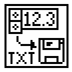

Write To Spreadsheet File.vi
C:\Program Files\National Instruments\LabVIEW 6 SE\vi.lib\Utility\file.llb\Write To Spreadsheet File.vi

History
"Thesis Prop.vi History"
Current Revision: 21

Position in Hierarchy

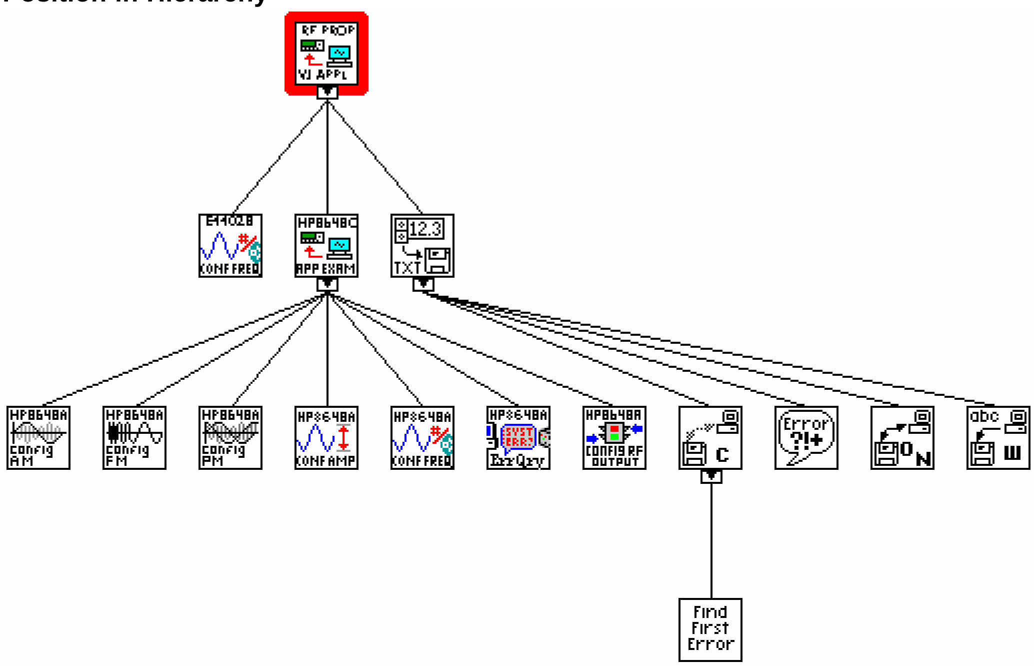

HP8648A Application Function.vi
This VI demonstrates how to combine different subVI's to form a higher level example. This application example configures amplitude, frequency and modulation. It also includes RF output on/off and error checking.

Connector Pane

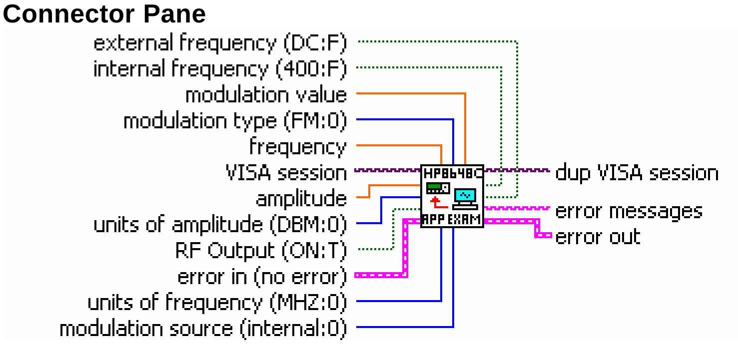

Controls and Indicators

error in (no error) The error in cluster can accept error information wired from VIs previously called. Use this information to decide if any functionality should be bypassed in the event of errors from other VIs.

The pop-up option Explain Error (or Explain Warning) gives more information about the error displayed.

status The status boolean is either TRUE (X) for an error, or FALSE (checkmark) for no error or a warning.

The pop-up option Explain Error (or Explain Warning) gives more information about the error displayed.

code The code input identifies the error or warning.

The pop-up option Explain Error (or Explain Warning) gives more information about the error displayed.

source The source string describes the origin of the error or warning.

The pop-up option Explain Error (or Explain Warning) gives more information about the error displayed.

amplitude Sets the amplitude of the RF output to the desired value. This value may be up to 4 digits plus a sign if applicable, e.g. -127.1 or maximum resolution of .1 dB, .001 mV, .01 uV. The RF output amplitude range is -136 dBm to +10 dBm with over range to +13 dBm.

When making amplitude changes, the instrument does not turn off the RF Output. The electronic attenuator provides rapid amplitude changes. The period of any over- or under-ranging that may occur during level transitions is typically less than 30 ms.

units of amplitude (DBM:0) Sets the units of amplitude. Units may be:

0 - DBM
1 - MV
2 - UV
3 - MVEMF
4 - UVEMF
5 - DBUV
6 - DBUVEMF

Note: If in reference mode, only DBM is allowed.

frequency Sets the RF frequency to the entered value. The value may be up to 9 digits with a maximum of 10 Hz resolution.
The RF output frequency range is 250 kHz to 1000 MHz.

When making frequency changes, the instrument does not turn off the RF Output. Frequency switching typically takes less than 100 ms. Worst case conditions occur for changes which cross the instrument's two frequency bands (249 MHz and 501 MHz).

units of frequency (MHZ:0) Sets the units of frequency. Units may be:

0 - MHZ, megahertz
1 - KHZ, kilohertz

2 - HZ, hertz

modulation value Sets the corresponding modulation value.

If the modulation type is FM, the value represents FM deviation in kilohertz. The FM deviation range is 0.00 to 99.9 kHz.

If the modulation type is AM, the value represents AM depth in percent. The AM depth range is .1 to 99.9 percent.

If the modulation type is PM, the value represents PM deviation in radians. The PM deviation range is 0.00 to 10.0 radians

modulation source (internal:0) Selects the frequency modulation source. The internal sources can have either 1 kHz or 400 Hz frequencies. The external source can be AC or DC coupled for FM or AC coupled only for AM and PM. These options are set by the controls below.

0 - internal source
1 - external source
2 - both internal and external sources

internal frequency (400:F) Selects the internal frequency.

T - 1 kHz frequency
F - 400 Hz frequency

external frequency (DC:F) Selects the FM external coupling.

T - external AC coupling for FM
F - external DC coupling for FM

This control is ignored when the modulation type is AM or PM.

modulation type (FM:0) Selects the type of modulation.

0 - FM; frequency modulation
1 - AM; aplitude modulation
2 - PM; phase modulation

RF Output (ON:T) Turns the RF output on and off.

T - RF output on
F - RF output off

VISA session

error out The error out cluster passes error or warning information out of a VI to be used by other VIs.

The pop-up option Explain Error (or Explain Warning) gives more information about the error displayed.

status The status boolean is either TRUE (X) for an error, or FALSE (checkmark) for no error or a warning.

The pop-up option Explain Error (or Explain Warning) gives more information about the error displayed.

code The code input identifies the error or warning.

The pop-up option Explain Error (or Explain Warning) gives more information about the error displayed.

source The source string describes the origin of the error or warning.

The pop-up option Explain Error (or Explain Warning) gives more information about the error displayed.

dup VISA session

error messages

E4402B Configure Frequency.vi
This VI configures the start and stop frequencies. The frequency range is 9 kHz to 3.0 GHz.

Connector Pane

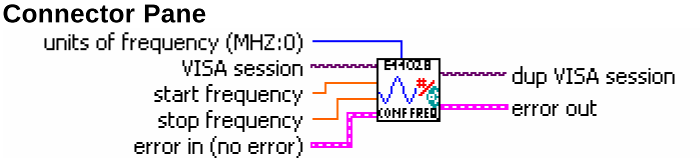

Controls and Indicators

VISA session

error in (no error) The error in cluster can accept error information wired from VIs previously called. Use this information to decide if any functionality should be bypassed in the event of errors from other VIs.

The pop-up option Explain Error (or Explain Warning) gives more information about the error displayed.

status The status boolean is either TRUE (X) for an error, or FALSE (checkmark) for no error or a warning.

The pop-up option Explain Error (or Explain Warning) gives more information about the error displayed.

code The code input identifies the error or warning.

The pop-up option Explain Error (or Explain Warning) gives more information about the error displayed.

source The source string describes the origin of the error or warning.

The pop-up option Explain Error (or Explain Warning) gives more information about the error displayed.

DBL **start frequency** Sets the RF frequency to the entered value. The value may be up to 9 digits with a maximum of 10 Hz resolution.
The RF output frequency range is 100 kHz to 1000 MHz.
When making frequency changes, the instrument does not turn off the RF Output. Frequency switching typically takes less than 100 ms. Worst case conditions occur for changes which cross the instrument's two frequency bands (249 MHz and 501 MHz).

U16 **units of frequency (MHZ:0)** Sets the units of frequency. Units may be:

0 - MHZ, megahertz
1 - KHZ, kilohertz
2 - HZ, hertz

DBL **stop frequency** Sets the RF frequency to the entered value. The value may be up to 9 digits with a maximum of 10 Hz resolution.
The RF output frequency range is 100 kHz to 1000 MHz.
When making frequency changes, the instrument does not turn off the RF Output. Frequency switching typically takes less than 100 ms. Worst case conditions occur for changes which cross the instrument's two frequency bands (249 MHz and 501 MHz).

error out The error out cluster passes error or warning information out of a VI to be used by other VIs.

The pop-up option Explain Error (or Explain Warning) gives more information about the error displayed.

TF **status** The status boolean is either TRUE (X) for an error, or FALSE (checkmark) for no error or a warning.

The pop-up option Explain Error (or Explain Warning) gives more information about the error displayed.

I32 **code** The code input identifies the error or warning.

The pop-up option Explain Error (or Explain Warning) gives more information about the error displayed.

abc **source** The source string describes the origin of the error or warning.

The pop-up option Explain Error (or Explain Warning) gives more information about the error displayed.

I/O **dup VISA session**

APPENDIX B

DATA LOG SHEETS

4/18/2002 Record testing

Date	Time	Temp	R/H	Material		Test Trial	Saved
4/18	9:33A	77°	68%	Air	000	01	✓
4/18	9:41A	77°	68%	Air	030	01	✓
4/18	9:45A	77°	68%	Air	060	01	✓
4/18	9:49A	77°	68%	Air	090	01	✓
4/18	9:53A	78°	68%	Air	120	01	✓
4/18	9:57A	78°	68%	Air	150	01	✓
4/18	10:01A	78°	68%	Air	180	01	✓
4/18	10:04A	78°	68%	Air	180	02	✓
4/18	10:09A	78°	68%	Air	150	02	✓
4/18	10:13A	78°	68%	Air	120	02	✓
4/18	10:17A	78°	68%	Air	090	02	✓
4/18	10:20A	78°	67%	Air	060	02	✓
4/18	10:24A	78°	67%	Air	030	02	✓
4/18	10:28A	78°	67%	Air	000	02	✓
4/18	10:31A	78°	65%	Air	000	03	✓
4/18	10:35A	78°	65%	Air	030	03	✓
4/18	10:39A	78°	65%	Air	060	03	✓
4/18	10:46A	79°	65%	Air	090	03	✓
4/18	10:58A	79°	65%	Air	120	03	✓
4/18	11:02A	79°	64%	Air	150	03	✓
4/18	11:05A	79°	64%	Air	180	03	✓
4/18	11:09A	79°	64%	Air	180	04	✓
4/18	11:12A	79°	64%	Air	150	04	✓
4/18	11:16A	79°	64%	Air	120	04	✓
4/18	11:20A	79°	64%	Air	090	04	✓
4/18	11:23A	79°	64%	Air	060	04	✓
4/18	11:27A	79°	64%	Air	030	04	✓
4/18	11:31A	79°	64%	Air	000	04	✓
4/18	11:34A	79°	64%	Air	000	05	✓
4/18	11:38A	79°	63%	Air	030	05	✓
4/18	11:42A	79°	63%	Air	060	05	✓
4/18	11:46A	79°	63%	Air	090	05	✓

Files naming convention =

material _ date _ iteration _ X

so:

air _ 041802 _ 01 _ 000.xls

sty - 041802 _ 05 _ -090.xls

Date	Time	Temp	R/H	Material	X	Test Trial	saved
4/18	11:49A	79°	63%	Air	120	05	✓
4/18	11:53A	79°	63%	Air	150	05	✓
4/18	11:56A	79°	63%	Air	180	05	✓
4/18	12:04p	79°	63%	Sty 3/4"	000	01	✓
4/18	12:08p	79°	63%	Sty w/Film	030	01	✓
4/18	12:13p	79°	63%	sty	060	01	✓
4/18	12:17p	79°	63%	sty	090	01	✓
4/18	12:23p	79°	62%	sty	120	01	✓
4/18	12:27p	79°	62%	sty	150	01	✓
4/18	12:31p	79°	62%	sty	180	01	✓
4/18	12:34p	79°	62%	sty	180	02	✓
4/18	12:38p	79°	62%	sty	150	02	✓
4/18	12:42p	79°	62%	sty	120	02	✓
4/18	12:45p	79°	62%	sty	090	02	✓
4/18	12:49p	79°	62%	sty	060	02	✓
4/18	12:53p	79°	62%	sty	030	02	✓
4/18	12:56p	79°	62%	sty	000	02	✓
4/18	1:00p	79°	62%	sty	000	03	✓
4/18	1:04p	79°	62%	sty	030	03	✓
4/18	1:08p	79°	62%	sty	060	03	✓
4/18	1:11p	79°	62%	sty	090	03	✓
4/18	1:15p	79°	62%	sty	120	03	✓
4/18	1:19p	79°	61%	sty	150	03	✓
4/18	1:23p	79°	61%	sty	180	03	✓
4/18	1:26p	79°	61%	sty	180	04	✓

Date	Time	Temp	R/H	Material	∡	Test Trial	Saved
4/18	1:30p	79°	61%	Sty	150	04	✓
4/18	1:34p	79°	61%	Sty	120	04	✓
4/18	1:37p	79°	61%	Sty	090	04	✓
4/18	1:41p	79°	61%	Sty	060	04	✓
4/18	1:45p	79°	61%	Sty	030	04	✓
4/18	1:48p	79°	61%	Sty	000	04	✓
4/18	1:52p	79°	61%	Sty	000	05	✓
4/18	1:55p	79°	61%	Sty	030	05	✓
4/18	1:59p	79°	61%	Sty	060	05	✓
4/18	2:03p	79°	61%	Sty	090	05	✓
4/18	2:07p	79°	61%	Sty	120	05	✓
4/18	2:10p	79°	61%	Sty	150	05	✓
4/18	2:14p	79°	61%	Sty	180	05	✓
4/18	2:24p	79°	61%	Lex	000	01	✓
4/18	2:27p	79°	61%	Lex	030	01	✓
4/18	2:31p	79°	61%	Lex	060	01	✓
4/18	2:36p	79°	61%	Lex	090	01	✓
4/18	2:40p	79°	60%	Lex	120	01	✓
4/18	2:43p	79°	60%	Lex	150	01	✓
4/18	2:47p	79°	60%	Lex	180	01	✓
4/18	2:50p	79°	60%	Lex	180	02	✓
4/18	2:54p	79°	60%	Lex	150	02	✓
4/18	2:58p	79°	60%	Lex	120	02	✓
4/18	3:02p	79°	60%	Lex	090	02	✓
4/18	3:07p	79°	60%	Lex	060	02	✓
4/18	3:12p	79°	60%	Lex	030	02	✓
4/18	3:16p	79°	60%	Lex	000	02	✓
4/18	3:20p	79°	60%	Lex	000	03	✓
4/18	3:23p	79°	60%	Lex	030	03	✓
4/18	3:27p	79°	60%	Lex	060	03	✓
4/18	3:31p	79°	60%	Lex	090	03	✓
4/18	3:34p	79°	60%	Lex	120	03	✓
4/18	3:38p	79°	60%	Lex	150	03	✓

Date	Time	Temp	RH	Material	∠	Test Trial	Saved
4/18	3:42p	79°	60%	Lex	180	03	✓
4/18	3:45p	79°	60%	Lex	180	04	✓
4/18	3:49p	79°	60%	Lex	150	04	✓
4/18	3:52p	79°	60%	Lex	120	04	✓
4/18	3:56p	79°	60%	Lex	090	04	✓
4/18	4:00p	79°	60%	Lex	060	04	✓
4/18	4:04p	79°	60%	Lex	030	04	✓
4/18	4:08p	79°	60%	Lex	000	04	✓
4/18	4:11p	79°	60%	Lex	000	05	✓
4/18	4:15p	79°	60%	Lex	030	05	✓
4/18	4:19p	79°	60%	Lex	060	05	✓
4/18	4:23p	79°	60%	Lex	090	05	✓
4/18	4:26p	79°	60%	Lex	120	05	✓
4/18	4:30p	79°	60%	Lex	150	05	✓
4/18	4:34p	79°	60%	Lex	180	05	✓
4/19	8:05a	77°	68%	Tuf	000	01	✓
4/19	8:10a	77°	68%	Tuf	030	01	✓
4/19	8:14a	77°	68%	Tuf	060	01	✓
4/19	8:17a	78°	67%	Tuf	090	01	✓
4/19	8:21a	78°	67%	Tuf	120	01	✓
4/19	8:24a	78°	67%	Tuf	150	01	✓
4/19	8:28a	78°	67%	Tuf	180	01	✓
4/19	8:31a	78°	67%	Tuf	180	02	✓
4/19	8:35a	78°	66%	Tuf	150	02	✓
4/19	8:39a	78°	66%	Tuf	120	02	✓
4/19	8:42a	78°	66%	Tuf	090	02	✓
4/19	8:46a	78°	65%	Tuf	060	02	✓
4/19	8:50a	78°	65%	Tuf	030	02	✓
4/19	8:53a	78°	65%	Tuf	000	02	✓
4/19	8:57a	78°	64%	Tuf	000	03	✓
4/19	9:00a	78°	64%	Tuf	030	03	✓
4/19	9:04a	78°	64%	Tuf	060	03	✓
4/19	9:08a	78°	64%	Tuf	090	03	✓

Date	Time	Temp	RH	Material	X	Test Trial	Saved
4/19	9:12a	78°	63%	Tuf	120	03	✓
4/19	9:15a	78°	63%	Tuf	150	03	✓
4/19	9:19a	78°	63%	Tuf	180	03	✓
4/19	9:22a	78°	63%	Tuf	180	04	✓
4/19	9:26a	78°	63%	Tuf	150	04	✓
4/19	9:30a	78°	63%	Tuf	120	04	✓
4/19	9:33a	78°	63%	Tuf	090	04	✓
4/19	9:37a	79°	62%	Tuf	060	04	✓
4/19	9:41a	79°	62%	Tuf	030	04	✓
4/19	9:44a	79°	62%	Tuf	000	04	✓
4/19	9:48a	79°	62%	Tuf	000	05	✓
4/19	9:51a	79°	62%	Tuf	030	05	✓
4/19	9:55a	79°	62%	Tuf	060	05	✓
4/19	9:59a	79°	62%	Tuf	090	05	✓
4/19	10:02a	79°	62%	Tuf	120	05	✓
4/19	10:06a	79°	62%	Tuf	150	05	✓
4/19	10:09a	79°	62%	Tuf	180	05	✓
4/19	10:16a	79°	62%	Air 2	000	01	✓
4/19	10:21a	79°	62%	Air 2	030	01	✓
4/19	10:24a	79°	62%	Air 2	060	01	✓
4/19	10:27a	79°	62%	Air 2	090	01	✓
4/19	10:31a	79°	62%	Air 2	120	01	✓
4/19	10:34a	79°	62%	Air 2	150	01	✓
4/19	10:38a	79°	62%	Air 2	180	01	✓
4/19	10:41a	79°	61%	Air 2	180	02	✓
4/19	10:45a	79°	61%	Air 2	150	02	✓
4/19	10:48a	79°	61%	Air 2	120	02	✓
4/19	10:52a	79°	61%	Air 2	090	02	✓
4/19	10:56a	79°	61%	Air 2	060	02	✓
4/19	10:59a	79°	61%	Air 2	030	02	✓
4/19	11:03a	79°	61%	Air 2	000	02	✓
4/19	11:06a	79°	61%	Air 2	000	03	✓
4/19	11:10a	79°	61%	Air 2	030	03	✓

Date	Time	Temp	RH	Material	∡	Test Trial	Saved
4/19	11:16a	79°	61%	Air 2	060	03	✓
4/19	11:18a	79°	61%	Air 2	090	03	✓
4/19	11:22a	79°	61%	Air 2	120	03	✓
4/19	11:26a	79°	61%	Air 2	150	03	✓
4/19	11:29a	79°	61%	Air 2	180	03	✓
4/19	11:32a	79°	61%	Air 2	180	04	✓
4/19	11:36a	79°	61%	Air 2	150	04	✓
4/19	11:40a	79°	61%	Air 2	120	04	✓
4/19	11:43a	79°	61%	Air 2	090	04	✓
4/19	11:47a	79°	61%	Air 2	060	04	✓
4/19	11:51a	79°	61%	Air 2	030	04	✓
4/19	11:54a	79°	61%	Air 2	000	04	✓
4/19	11:57a	79°	61%	Air 2	000	05	✓
4/19	12:01p	79°	61%	Air 2	030	05	✓
4/19	12:10p	79°	61%	Air 2	060	05	✓
4/19	12:13p	79°	61%	Air 2	090	05	✓
4/19	12:17p	79°	61%	Air 2	120	05	✓
4/19	12:20p	79°	61%	Air 2	150	05	✓
4/19	12:24p	79°	61%	Air 2	180	05	✓

APPENDIX C

SAMPLE OF EXPERIMENTAL DATA

air1_041802_01_-090

1850	1855	1860	1865	1870	1875	1880	1885	1890	1895	1900	1905	1910	1915	1920	1925	1930	1935	1940	1945	1950	1955	1960	1965	1970	1975	1980	1985	1990
-41.73	-42.25	-43.64	-43.45	-40.45	-45.06	-47.12	-47.31	-48.39	-43.91	-60.75	-48.28	-44.84	-41.69	-43.42	-49.73	-51.95	-53.83	-44.57	-51.20	-39.10	-46.62	-43.89	-48.41	-45.25	-46.92	-42.82	-45.79	-42.70
-41.73	-42.53	-43.93	-43.38	-40.51	-45.41	-47.10	-47.67	-47.94	-44.20	-60.39	-48.55	-44.38	-41.80	-43.42	-49.59	-52.45	-55.19	-44.33	-51.00	-39.01	-46.77	-43.82	-47.99	-45.57	-46.87	-42.82	-45.68	-42.87
-41.74	-42.25	-43.88	-43.44	-40.86	-45.27	-46.65	-47.49	-48.34	-44.02	-61.60	-48.52	-44.82	-41.64	-43.14	-49.53	-51.65	-54.26	-44.43	-50.86	-38.95	-46.66	-43.76	-48.60	-45.10	-46.84	-42.64	-45.69	-42.82
-41.76	-42.25	-43.86	-43.41	-40.87	-45.38	-47.02	-47.57	-47.46	-44.15	-60.38	-48.03	-44.89	-41.67	-43.19	-49.55	-52.21	-54.35	-44.68	-51.26	-38.99	-46.88	-43.62	-47.99	-45.10	-46.56	-42.66	-45.83	-42.89
-41.88	-42.08	-43.92	-43.26	-40.37	-45.27	-47.11	-47.26	-47.92	-44.09	-60.97	-48.18	-45.09	-41.80	-43.32	-49.11	-52.33	-54.81	-44.19	-50.80	-38.97	-46.53	-43.45	-48.40	-45.04	-46.79	-42.92	-45.55	-43.20
-41.68	-42.12	-43.98	-43.55	-40.51	-45.22	-46.71	-47.31	-48.08	-44.34	-60.34	-48.03	-44.84	-42.24	-43.69	-49.26	-51.89	-55.07	-44.60	-51.47	-38.97	-46.60	-43.77	-47.99	-45.58	-46.92	-42.74	-45.71	-42.90
-41.52	-42.52	-43.90	-43.41	-40.64	-45.38	-46.97	-47.21	-48.27	-44.17	-60.97	-48.32	-44.45	-41.91	-43.20	-48.90	-52.31	-54.31	-44.49	-51.48	-38.71	-46.38	-43.71	-48.75	-45.43	-46.52	-42.77	-45.87	-42.81
-41.55	-42.33	-43.97	-42.96	-40.55	-45.48	-47.18	-47.36	-48.57	-44.04	-61.52	-48.14	-44.86	-41.65	-43.43	-49.34	-51.66	-54.36	-44.23	-50.73	-38.86	-46.52	-43.81	-48.23	-45.44	-46.85	-42.54	-45.68	-42.92
-42.06	-42.53	-44.13	-43.17	-40.41	-45.20	-46.59	-47.12	-47.38	-44.08	-60.98	-48.50	-44.77	-41.49	-43.41	-49.36	-52.13	-54.54	-44.41	-51.69	-38.94	-46.54	-43.35	-48.25	-44.90	-46.90	-42.74	-45.45	-42.88
-41.68	-42.50	-43.74	-43.23	-40.57	-45.13	-46.63	-47.09	-47.64	-43.95	-60.50	-48.22	-44.86	-41.80	-43.29	-49.22	-51.67	-55.01	-44.61	-51.22	-38.94	-46.02	-43.87	-48.55	-45.46	-46.75	-42.60	-45.43	-42.86
-41.69	-42.32	-43.93	-43.19	-40.50	-45.19	-46.99	-47.40	-48.05	-43.95	-60.50	-47.83	-45.13	-41.95	-43.22	-49.11	-51.13	-54.62	-44.35	-51.06	-38.75	-46.18	-43.64	-48.22	-45.12	-46.46	-42.76	-45.82	-42.95
-41.41	-42.25	-43.84	-43.33	-40.62	-45.06	-46.50	-47.27	-47.41	-43.86	-61.28	-48.33	-44.90	-41.96	-43.41	-49.39	-52.28	-55.36	-44.41	-50.82	-39.01	-46.24	-43.64	-48.26	-45.35	-46.82	-42.71	-45.89	-43.03
-41.83	-42.41	-43.87	-43.07	-40.53	-45.32	-46.96	-47.83	-48.53	-44.04	-60.08	-47.77	-44.84	-41.78	-43.18	-49.46	-51.50	-54.09	-44.53	-50.93	-38.92	-46.81	-43.92	-48.44	-45.09	-46.31	-42.88	-45.61	-43.03
-41.54	-42.39	-43.71	-43.21	-40.62	-45.11	-46.76	-47.57	-47.57	-44.10	-61.38	-48.13	-45.19	-41.92	-43.43	-49.23	-51.74	-54.91	-44.50	-51.22	-38.70	-46.64	-43.61	-48.08	-45.46	-46.82	-42.63	-45.81	-42.93
-41.98	-42.10	-43.94	-43.21	-40.57	-45.18	-46.89	-47.02	-47.77	-44.05	-61.59	-48.52	-44.77	-41.84	-43.34	-49.43	-52.36	-54.14	-44.27	-51.22	-38.90	-46.64	-43.80	-48.38	-45.42	-46.44	-42.52	-45.90	-42.90
-41.65	-42.10	-43.67	-43.33	-40.58	-45.31	-46.79	-47.26	-48.27	-43.75	-60.19	-48.44	-44.70	-41.82	-43.45	-49.49	-52.02	-55.70	-44.37	-50.82	-38.96	-46.57	-43.75	-48.31	-45.34	-46.56	-42.65	-45.96	-42.97
-41.73	-42.55	-44.03	-43.25	-40.43	-45.23	-46.99	-47.32	-47.93	-43.91	-60.97	-48.10	-44.92	-41.96	-43.36	-49.94	-51.57	-54.38	-44.43	-51.34	-38.87	-46.79	-43.71	-48.32	-45.36	-47.05	-42.48	-45.68	-42.89
-41.68	-42.34	-43.78	-43.46	-40.39	-45.07	-46.75	-47.32	-47.95	-44.07	-59.81	-47.91	-44.97	-41.83	-43.68	-49.58	-52.57	-54.38	-44.45	-50.84	-38.92	-46.87	-43.75	-48.13	-45.16	-46.60	-42.73	-45.46	-42.91
-41.60	-42.12	-43.79	-43.55	-40.73	-45.13	-46.71	-47.10	-48.19	-44.09	-60.58	-48.49	-44.87	-42.08	-43.29	-49.87	-51.66	-54.91	-44.12	-50.91	-38.90	-46.65	-43.54	-48.50	-45.49	-46.41	-42.59	-45.78	-43.02
-41.59	-42.38	-43.75	-43.43	-40.75	-45.38	-46.86	-47.13	-48.09	-43.93	-61.35	-48.25	-44.72	-42.02	-43.32	-49.94	-52.17	-55.44	-44.12	-51.11	-38.84	-46.72	-43.69	-47.91	-45.35	-46.56	-42.82	-45.37	-42.52
-41.79	-42.11	-43.53	-43.28	-40.51	-45.29	-47.07	-47.50	-47.33	-44.02	-60.47	-47.99	-44.91	-41.94	-43.43	-49.58	-51.92	-54.96	-44.57	-50.83	-39.04	-46.74	-43.79	-48.41	-45.13	-46.80	-42.76	-45.93	-43.11
-41.79	-42.31	-43.74	-43.23	-40.66	-45.13	-46.59	-47.59	-48.24	-44.25	-61.40	-48.48	-44.82	-41.67	-43.14	-48.67	-52.04	-54.32	-44.38	-51.17	-39.06	-46.46	-43.59	-48.88	-45.04	-46.67	-42.54	-45.59	-43.07
-41.75	-42.60	-43.88	-43.38	-40.48	-45.53	-46.97	-47.20	-48.38	-43.79	-59.66	-48.42	-45.05	-41.95	-43.53	-49.39	-51.61	-53.97	-44.33	-51.48	-38.82	-46.62	-43.91	-48.88	-45.52	-46.75	-42.54	-45.31	-42.80
-41.77	-42.30	-43.97	-43.21	-40.56	-45.40	-46.72	-47.23	-48.35	-44.08	-60.84	-48.19	-44.80	-41.82	-43.54	-49.68	-52.30	-54.30	-44.10	-51.26	-38.92	-46.59	-43.83	-48.58	-45.36	-46.94	-42.95	-45.84	-43.17
-41.68	-42.47	-43.68	-43.16	-40.77	-45.41	-46.74	-47.65	-47.94	-44.20	-60.83	-48.21	-44.87	-41.78	-43.46	-49.37	-52.74	-54.75	-44.27	-51.11	-38.92	-46.60	-43.89	-47.89	-44.96	-46.27	-42.93	-45.82	-42.88
-41.76	-42.51	-43.74	-43.45	-40.66	-45.18	-46.85	-47.17	-47.83	-43.83	-60.88	-48.43	-44.98	-41.71	-43.63	-49.91	-52.13	-54.73	-44.58	-50.42	-38.98	-46.65	-43.52	-47.86	-45.10	-46.94	-42.35	-45.66	-42.93
-41.58	-42.37	-43.70	-43.45	-40.37	-45.31	-46.92	-47.41	-48.25	-43.84	-60.98	-48.61	-44.69	-41.99	-43.54	-49.19	-52.15	-54.40	-44.54	-51.87	-38.91	-46.65	-43.99	-48.08	-45.35	-46.22	-42.54	-46.16	-42.99
-41.65	-42.37	-43.97	-43.44	-40.75	-45.31	-46.79	-47.13	-48.23	-44.17	-60.52	-47.53	-44.95	-41.94	-43.18	-49.19	-52.19	-54.74	-44.39	-50.83	-39.11	-46.35	-43.79	-48.67	-45.18	-46.30	-42.87	-46.25	-43.02
-41.83	-42.21	-43.82	-43.00	-40.68	-45.21	-46.96	-47.33	-47.78	-43.70	-60.87	-47.75	-45.19	-41.79	-43.45	-49.04	-51.42	-54.85	-44.33	-51.21	-38.96	-46.88	-43.79	-48.60	-45.32	-46.76	-42.45	-45.78	-42.90
-41.69	-42.22	-43.63	-43.20	-40.60	-45.15	-46.88	-47.34	-47.62	-44.07	-59.65	-48.40	-44.76	-41.87	-43.36	-49.12	-51.42	-54.25	-44.22	-51.82	-39.11	-46.10	-43.96	-48.37	-45.60	-46.73	-42.52	-45.77	-43.05
-41.71	-42.41	-43.59	-43.20	-40.61	-45.34	-47.09	-47.75	-47.92	-44.13	-60.01	-48.11	-44.97	-41.98	-43.51	-49.64	-52.27	-54.57	-44.46	-50.18	-39.02	-46.90	-43.79	-48.37	-45.50	-46.38	-42.46	-45.75	-42.80
-41.90	-42.27	-44.04	-43.10	-40.49	-45.22	-46.96	-47.55	-48.61	-44.23	-59.72	-48.32	-45.16	-41.63	-43.36	-49.42	-52.44	-55.17	-44.54	-50.88	-38.95	-46.70	-43.69	-48.48	-45.12	-46.60	-42.86	-45.81	-42.94
-41.82	-42.43	-43.83	-43.40	-40.56	-44.96	-47.13	-47.65	-48.19	-43.88	-60.22	-47.78	-44.73	-41.97	-43.54	-49.10	-52.24	-54.29	-44.40	-51.53	-39.05	-46.76	-44.04	-47.98	-45.12	-46.25	-42.55	-46.20	-43.09
-41.65	-42.14	-43.63	-43.23	-40.77	-45.45	-47.18	-47.17	-47.83	-43.93	-59.19	-47.97	-44.96	-41.80	-43.43	-49.32	-52.11	-54.99	-44.67	-51.03	-38.94	-46.71	-43.70	-48.04	-45.23	-46.84	-42.85	-45.66	-42.90
-41.63	-42.37	-43.75	-43.41	-40.48	-45.23	-46.93	-47.40	-47.87	-44.12	-60.77	-48.48	-44.74	-42.12	-43.50	-49.15	-52.42	-55.27	-44.54	-50.78	-38.99	-46.66	-43.80	-48.60	-45.78	-46.78	-42.66	-45.61	-43.12
-41.57	-42.39	-43.84	-43.17	-40.74	-45.39	-46.94	-47.13	-48.34	-43.99	-61.44	-48.37	-44.87	-41.97	-43.53	-49.13	-52.17	-54.62	-44.39	-51.12	-38.82	-46.66	-43.75	-48.02	-45.55	-46.55	-42.74	-45.64	-42.71
-41.81	-42.11	-43.98	-43.38	-40.65	-45.36	-46.93	-47.29	-48.46	-44.09	-61.45	-48.38	-44.93	-41.78	-43.26	-49.41	-52.62	-54.98	-44.55	-51.12	-38.82	-46.93	-43.59	-48.50	-45.37	-46.85	-42.77	-45.84	-42.78
-41.79	-42.05	-43.89	-43.04	-40.79	-45.51	-46.88	-47.08	-47.82	-44.18	-61.23	-48.67	-44.75	-41.97	-43.44	-49.76	-52.27	-54.90	-44.13	-51.06	-38.89	-46.85	-43.42	-48.33	-45.32	-46.62	-42.58	-45.77	-43.14
-41.71	-41.86	-43.89	-43.04	-40.78	-45.15	-47.12	-47.46	-47.86	-44.02	-61.22	-48.21	-44.79	-41.59	-43.47	-49.10	-51.88	-55.03	-44.34	-50.44	-38.64	-46.42	-43.89	-47.80	-45.45	-46.52	-42.62	-45.60	-43.33
-41.76	-41.86	-43.89	-43.29	-40.63	-44.95	-47.15	-47.57	-47.93	-44.15	-60.67	-48.33	-44.80	-41.84	-43.29	-49.29	-51.71	-55.09	-44.16	-51.20	-39.09	-47.02	-43.96	-48.47	-45.39	-46.59	-42.64	-45.60	-42.87

APPENDIX D

STATISTICAL ANALYSIS TABLES

Trials - Air	-90	-60	-30	0	30	60	90
1	-45.54	-43.80	-42.01	-38.91	-38.66	-43.83	-46.87
2	-45.43	-43.76	-41.87	-38.89	-38.67	-44.21	-46.89
3	-45.44	-43.75	-42.03	-38.89	-38.80	-44.15	-46.90
4	-45.27	-43.71	-41.86	-38.82	-38.82	-44.26	-46.92
5	-45.27	-43.76	-42.16	-38.88	-38.69	-44.34	-47.05

ANOVA: Two-Factor Without Replication

SUMMARY	*Count*	*Sum*	*Average*	*Variance*
1	7	-299.61	-42.80	9.84
2	7	-299.73	-42.82	9.96
3	7	-299.96	-42.85	9.74
4	7	-299.66	-42.81	9.77
5	7	-300.15	-42.88	10.00
-90	5	-226.95	-45.39	0.01
-60	5	-218.78	-43.76	0.00
-30	5	-209.93	-41.99	0.02
0	5	-194.39	-38.88	0.00
30	5	-193.64	-38.73	0.01
60	5	-220.79	-44.16	0.04
90	5	-234.63	-46.93	0.01

ANOVA

Source of Variation	*SS*	*df*	*MS*	*F*	*P-value*	*F crit*
Trial	0.03	4	0.01	0.59	0.67	2.78
Angle of Incidence	295.62	6	49.27	3967.51	0.00	2.51
Error	0.30	24	0.01			
Total	295.95	34				

Trials - Styrofoam	-90	-60	-30	0	30	60	90
1	-46.35	-43.90	-41.35	-39.03	-38.92	-44.23	-46.77
2	-46.26	-43.75	-41.16	-38.99	-38.77	-44.50	-46.70
3	-46.23	-43.68	-41.88	-39.00	-38.68	-44.23	-46.61
4	-46.20	-44.04	-41.68	-39.02	-38.73	-44.64	-46.61
5	-46.18	-43.87	-42.06	-38.95	-38.66	-44.32	-46.65

ANOVA: Two-Factor Without Replication

SUMMARY	*Count*	*Sum*	*Average*	*Variance*
1	7	-300.56	-42.94	10.47
2	7	-300.13	-42.88	10.73
3	7	-300.31	-42.90	10.21
4	7	-300.93	-42.99	10.47
5	7	-300.69	-42.96	10.34
-90	5	-231.22	-46.24	0.00
-60	5	-219.24	-43.85	0.02
-30	5	-208.14	-41.63	0.14
0	5	-194.99	-39.00	0.00
30	5	-193.76	-38.75	0.01
60	5	-221.92	-44.38	0.03
90	5	-233.34	-46.67	0.00

ANOVA

Source of Variation	*SS*	*df*	*MS*	*F*	*P-value*	*F crit*
Trial	0.06	4	0.01	0.42	0.79	2.78
Angle of Incidence	312.54	6	52.09	1574.91	0.00	2.51
Error	0.79	24	0.03			
Total	313.39	34				

Trials - Lexan	-90	-60	-30	0	30	60	90
1	-44.88	-44.17	-43.15	-38.99	-39.26	-43.08	-46.31
2	-44.88	-44.39	-42.64	-38.86	-39.39	-42.75	-46.33
3	-44.86	-44.26	-42.72	-39.13	-39.56	-43.10	-46.15
4	-44.48	-44.23	-42.79	-38.97	-39.55	-43.17	-46.16
5	-44.48	-43.88	-42.68	-38.98	-39.29	-43.11	-46.29

ANOVA: Two-Factor Without Replication

SUMMARY	*Count*	*Sum*	*Average*	*Variance*
1	7	-299.84	-42.83	7.63
2	7	-299.25	-42.75	7.75
3	7	-299.79	-42.83	6.94
4	7	-299.35	-42.76	6.92
5	7	-298.71	-42.67	7.19
-90	5	-223.59	-44.72	0.05

-60	5	-220.93	-44.19	0.04
-30	5	-213.98	-42.80	0.04
0	5	-194.92	-38.98	0.01
30	5	-197.05	-39.41	0.02
60	5	-215.22	-43.04	0.03
90	5	-231.24	-46.25	0.01

ANOVA

Source of Variation	*SS*	*df*	*MS*	*F*	*P-value*	*F crit*
Trial	0.12	4	0.03	1.16	0.36	2.78
Angle of Incidence	217.94	6	36.32	1386.34	0.00	2.51
Error	0.63	24	0.03			
Total	218.69	34				

Trials – Tuff Span	-90	-60	-30	0	30	60	90
1	-45.05	-43.89	-43.11	-39.95	-40.31	-42.86	-46.30
2	-44.97	-44.07	-43.01	-40.06	-40.40	-43.53	-46.31
3	-45.00	-44.20	-43.32	-40.03	-40.39	-43.11	-46.35
4	-44.94	-44.00	-43.21	-40.10	-40.42	-43.51	-46.37
5	-44.94	-44.08	-43.50	-40.18	-40.44	-42.97	-46.22

ANOVA: Two-Factor Without Replication

SUMMARY	*Count*	*Sum*	*Average*	*Variance*
1	7	-301.46	-43.07	5.41
2	7	-302.36	-43.19	5.23
3	7	-302.41	-43.20	5.35
4	7	-302.56	-43.22	5.19
5	7	-302.32	-43.19	4.97
-90	5	-224.90	-44.98	0.00
-60	5	-220.25	-44.05	0.01
-30	5	-216.15	-43.23	0.04
0	5	-200.32	-40.06	0.01
30	5	-201.96	-40.39	0.00
60	5	-215.97	-43.19	0.10
90	5	-231.55	-46.31	0.00

ANOVA

Source of Variation	*SS*	*df*	*MS*	*F*	*P-value*	*F crit*
Trial	0.11	4	0.03	1.23	0.33	2.78
Angle of Incidence	156.33	6	26.06	1177.27	0.00	2.51
Error	0.53	24	0.02			
Total	156.97	34				

APPENDIX E

TUKEY STATISTICAL ANALYSIS TABLES

The critical values of the studentized range (Q) distribution for the 95% confidence interval, 7 sample means and 21 degrees of freedom associated with MS(error):

Q (.05,7,21)=	4.62
w=	1.438689001

Air			Styrofoam		
Ranked Angle	Loss	Tukey significance	Ranked Angle	Loss	Tukey significance
0	-38.84067638		-30	-38.75296017	
-30	-38.9199169	0	0	-38.99819414	0
30	-41.96799483	-3.048077931	30	-41.62819828	-2.630004138
60	-44.21720345	-2.249208621	60	-43.84895914	-2.220760862
-60	-44.58478897	0	-60	-44.38453017	0
90	-46.11427069	-1.529481724	90	-46.24328897	-1.858758793
-90	-46.60243362	0	-90	-46.66732052	0

Lexan			Tuffspan		
Ranked Angle	Loss	Tukey significance	Ranked Angle	Loss	Tukey significance
0	-38.98464052		0	-40.06450034	
-30	-39.41033362	0	-30	-40.39296207	0
30	-42.79646448	-3.386130862	-60	-43.1936569	-2.800694828
-60	-43.04304466	0	30	-43.22968224	0
60	-44.18500672	0	60	-44.05062672	0
90	-44.71716328	0	90	-44.980095	0
-90	-46.24889793	-1.531734655	-90	-46.30915345	0

APPENDIX F

CALCULATIONS FOR BREWSTER'S ANGLE AND MATERIAL IMPEDANCES

Frequency (MHz)	Free Space Loss (L)	Transmit Power	Feeder Loss (LT)	Antenna Gain (GT)	Antenna Gain (GR)	Feeder Loss (LR)	Receive Power (PR)
1850	-19.78413455	10	1.785	8.4	8.4	1.785	43.01413455
1855	-19.76069084	10	1.785	8.4	8.4	1.785	42.99069084
1860	-19.73731024	10	1.785	8.4	8.4	1.785	42.96731024
1865	-19.7139924	10	1.785	8.4	8.4	1.785	42.9439924
1870	-19.69073699	10	1.785	8.4	8.4	1.785	42.92073699
1875	-19.66754368	10	1.785	8.4	8.4	1.785	42.89754368
1880	-19.64441214	10	1.785	8.4	8.4	1.785	42.87441214
1885	-19.62134203	10	1.785	8.4	8.4	1.785	42.85134203
1890	-19.59833304	10	1.785	8.4	8.4	1.785	42.82833304
1895	-19.57538483	10	1.785	8.4	8.4	1.785	42.80538483
1900	-19.5524971	10	1.785	8.4	8.4	1.785	42.7824971
1905	-19.52966952	10	1.785	8.4	8.4	1.785	42.75966952
1910	-19.50690178	10	1.785	8.4	8.4	1.785	42.73690178
1915	-19.48419355	10	1.785	8.4	8.4	1.785	42.71419355
1920	-19.46154455	10	1.785	8.4	8.4	1.785	42.69154455
1925	-19.43895444	10	1.785	8.4	8.4	1.785	42.66895444
1930	-19.41642294	10	1.785	8.4	8.4	1.785	42.64642294
1935	-19.39394973	10	1.785	8.4	8.4	1.785	42.62394973
1940	-19.37153452	10	1.785	8.4	8.4	1.785	42.60153452
1945	-19.34917701	10	1.785	8.4	8.4	1.785	42.57917701
1950	-19.32687689	10	1.785	8.4	8.4	1.785	42.55687689
1955	-19.30463389	10	1.785	8.4	8.4	1.785	42.53463389
1960	-19.28244769	10	1.785	8.4	8.4	1.785	42.51244769
1965	-19.26031803	10	1.785	8.4	8.4	1.785	42.49031803
1970	-19.2382446	10	1.785	8.4	8.4	1.785	42.4682446
1975	-19.21622712	10	1.785	8.4	8.4	1.785	42.44622712
1980	-19.19426532	10	1.785	8.4	8.4	1.785	42.42426532
1985	-19.1723589	10	1.785	8.4	8.4	1.785	42.4023589
1990	-19.15050759	10	1.785	8.4	8.4	1.785	42.38050759
							42.6936071

Frequency (MHz)	ω	νδ (στ)	νδ (αιρ)	*kd (st)*	*kd (air)*	w (st) - m	*ld (st)*	*ld (air)*
1920	3.0558E+08	1.8960E+08	2.9979E+08	1.6117	1.0193	0.0000	3.8986	6.1642

Angle of Incidence	Frequency (MHz)	Βω (στ)	cos(Bw*w) (st)	sin(Bw*w) (st)	Zin (st)	Γ (στ)	Τ (στ)	loss (st) - dB
0	1920	1.0193	1.0000000	0.0000000	377.0000	0.0000	1.0000	0.0000
30	1920	0.8827	1.0000000	0.0000000	435.3221	0.0718	1.0718	0.7180
60	1920	0.8058	1.0000000	0.0000000	754.0000	0.3333	1.3333	3.3333
90	1920	0.0000	1.0000000	0.0000000	1.0000E+99	1.0000	2.0000	10.0000

	Styro	Lexan	TuffSpan
Refractive, n	1.54	1.586	1.46
Dielectric, ε_r	2.5	2.96	4.8

Angle of Transmission within material

		Styro	Lexan	TuffSpan
Θ	Θ_R	Θ_T	Θ_T	Θ_T
0	0	0.00	0.00	0.00
30	30	18.97	17.44	13.69
60	60	37.95	34.87	27.39
90	90	56.92	52.31	41.08

Angle of Transmission within materials (radians)

		Styro	Lexan	TuffSpan
Θ	Θ_R	Θ_T	Θ_T	Θ_T
0	0	0	0	0
0.5235988	0.5235988	0.3311529	0.3043356	0.2389891
1.0471976	1.0471976	0.6623059	0.6086712	0.4779781
1.5707963	1.5707963	0.9934588	0.9130068	0.7169672

$\eta = 377 / \mathrm{sqrt}(\varepsilon_r)$

Styro	Lexan	TuffSpan	Air
238.43574	219.12680	172.07617	377.00000

Z_w^{TE}

Θ	Styro	Lexan	TuffSpan	Air
0	150.800	127.365	78.542	377.000
30	158.957	133.110	80.671	435.322
60	180.240	147.401	85.505	754.000
90	194.682	156.519	88.273	1.000E+99

Frequency (MHz)	ω	ν_d (st)	ν_d (lx)	ν_d (ts)	ν_d (air)
1920	3.0558E+08	1.8960E+08	1.7425E+08	1.3683E+08	2.9979E+08
		k_d (st)	k_d (lx)	k_d (ts)	k_d (air)
		1.6117	1.7537	2.2332	1.0193
		w (st) - m	w (lx) - m	w (ts) - m	
		0.0191	0.0024	0.0024	
		l_d (st)	l_d (lx)	l_d (ts)	l_d (air)
		3.8986	3.5829	2.8136	6.1642

Angle of Incidence	Frequency (MHz)	B_w (st)	B_w (lx)	B_w (ts)
0	1920	1.6117	1.7537	2.2332
30	1920	1.3957	1.5187	1.9340
60	1920	0.8058	0.8768	1.1166
90	1920	0.0000	0.0000	0.0000

$\cos(B_w$*w) (st)	$\cos(B_w$*w) (lx)	$\cos(B_w$*w) (ts)	$\sin(B_w$*w) (st)	$\sin(B_w$*w) (lx)	$\sin(B_w$*w) (ts)
0.9995287	0.9999914	0.9999861	0.0306974	0.0041425	0.0052752
0.9996465	0.9999936	0.9999896	0.0265857	0.0035875	0.0045685
0.9998822	0.9999979	0.9999965	0.0153505	0.0020713	0.0026376
1.0000000	1.0000000	1.0000000	0.0000000	0.0000000	0.0000000

Z_{in} (st)	Z_{in} (lx)	Z_{in} (ts)	Γ (st)	Γ (lx)	Γ (ts)
354.4192	372.9545	368.0937	-0.0309	-0.0054	-0.0120
409.7089	430.7458	425.2080	0.0416	0.0665	0.0601
711.0981	746.3971	737.0818	0.3070	0.3288	0.3232
1.0351E+20	7.6719E+20	6.0246E+20	1.0000	1.0000	1.0000

T (st)	T (lx)	T (ts)	loss (st) - dB	loss (lx) - dB	loss (ts) - dB
0.9691	0.9946	0.9880	0.3087	0.0539	0.1195
1.0416	1.0665	1.0601	0.4158	0.6654	0.6009
1.3070	1.3288	1.3232	3.0705	3.2882	3.2321
2.0000	2.0000	2.0000	10.0000	10.0000	10.0000

APPENDIX G

EQUIPMENT CALIBRATION CERTIFICATES

CERTIFIED TEST EQUIPMENT INC.

1314 South Shiloh Road, Garland, Texas 75042
Ph.972-494-9080 Fax 972-272-3889

CALIBRATION REPORT

Page 1/1

Report No: **2077-23**

Customer: **UNIVERSITY OF NORTH TEXAS**
Address: 1314 S. Shiloh Rd.
Garland, TX, 75042
Mfg/Model: **AGILENT TECHNOLOGIES E4402B**
Serial No: **US40241797**
ID No: **95051**
Calibration Interval as required by client: **1YR**
Calibration Date: **19MAR02**
Calibration Due Date: **19MAR03**
Technician: **EHO**
Procedure: Mfg. Specs.
Environmental Conditions: DEG F: **75** %RH: **47**

Test Instrument Found:

Within Tolerance: **X**
Component Failure:
Out of Tolerance:
Adjusted:
Other:

Remarks:

Standard Applied

C.T.E. certifies that the above instrument meets or exceeds all published specifications. It has been calibrated using standards whose accuracy are traceable to the National Institute of Standards and Technology, derived from accepted values of natural physical constants or have been derived by the ratio type of self-calibration techniquesThis document meets the requirements of the relevent purchase order, if applicable. The policies and procedures at C.T.E. comply with the intent of ISO/IEC 17025: 1999, ISO 9002: 1994, MIL-STD-45662A, and ANSI/NCSL Z540-1-1994 requirements and specifications. Calibration meets or exceeds 4:1 Accuracy Ratio unless otherwise noted in measurement data. Stated uncertainties are based on a coverage factor K=2 which gives a 95% confidence level. Results of measurements shown in this document relate only to the items calibrated.
NOTE: This report shall not be reproduced except in full, without the written approval of Certified Test Equipment

Standards Used in this Calibration:

Mfg/Model	Id. No.	Date Cal	Date Due
HP 5352B	1-5352	27 JAN 02	27 JUL 02
HP 436A	1-2925	03 NOV 01	03 MAY 02
HP 8481A	2-0103	10 MAY 01	10 MAY 02
NARDA 745-69	1-4760	16 OCT 01	16 OCT 02
HP 8406A	2-0129	06 NOV 01	06 MAY 02
HP 11581A	1-3420	14 SEP 01	14 SEP 02
HP 8620A	F6026	15 OCT 01	15 APR 02
HP 8660A	1-8092	08 DEC 01	08 JUN 02
HP 3311A	1-4527	06 NOV 01	06 MAY 02
HP 8484A	1-5518	19 SEP 01	19 SEP 02

Ralph Fundoots ___Ralph Fundoots___
Quality Manager

CTECALRPT-001 Rev. C

End of Report
12/07/01

Agilent Technologies	EPSG Order Fulfillment Operation FAsT C 1212 Valley House Drive Rohnert Park, CA 94928 (707) 794-1212

Certificate of Calibration

STANDARD CALIBRATION

Certificate No: 8648C3847A05252
Manufacturer: Agilent Technologies
Model No: 8648C
Options installed:

Description: Signal Generator
Serial No: 3847A05252

Date Calibrated: 26-Oct-2000
Temperature: 20-26 °C
Procedure Used: 8648C 26-OCT-2000

Humidity: 5-70% RH

This calibration certificate documents that the instrument identified above was calibrated under a quality system in compliance with requirements in ISO-9002 (1994), using applicable Agilent Technologies procedures.

As Received Condition: New
As Shipped Condition: This product meets published specifications

These calibration procedures and test points are those recommended in a procedure developed by Agilent. Performance verification during manufacturing may use measurement points that differ from an equivalent set described in published Agilent performance verification procedures.

Remarks or special requirements:

Traceability Information:
Agilent measurement standards are traceable to national standards, intrinsic standards, consensus standards, or by ratio type measurements. The national standards used by this lab are administered by NIST.

Documentation relative to specific traceability paths is on file and can be viewed as the calibration facility listed at the top of this page. This report shall not be reproduced, except in full, without prior written approval of the calibration facility.

Report Issued: 26-Oct-2000

Brad Brown
BRAD G. BROWN
INSPECTOR

5962-0476

APPENDIX H

CABLE TESTS GRAPHS

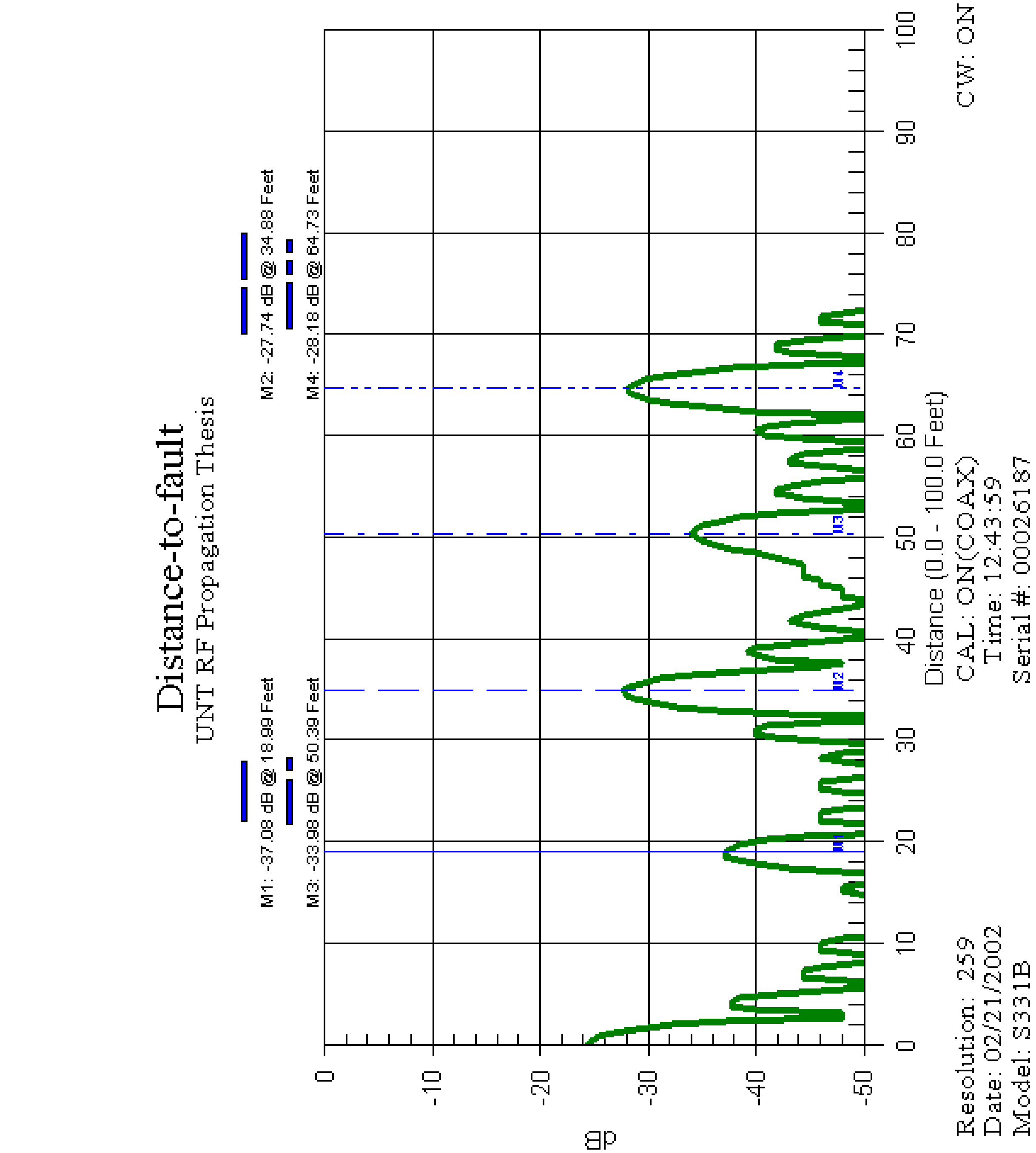
Distance-to-fault
UNT RF Propagation Thesis
M1: -37.08 dB @ 18.99 Feet
M2: -27.74 dB @ 34.88 Feet
M3: -33.98 dB @ 50.39 Feet
M4: -28.18 dB @ 64.73 Feet
dB
0
-10
-20
-30
-40
-50
0
10
20
30
40
50
60
70
80
90
100
Distance (0.0 - 100.0 Feet)
Resolution: 259
Date: 02/21/2002
Model: S331B
CAL: ON(COAX)
Time: 12:43:59
Serial #: 00026187
CW: ON

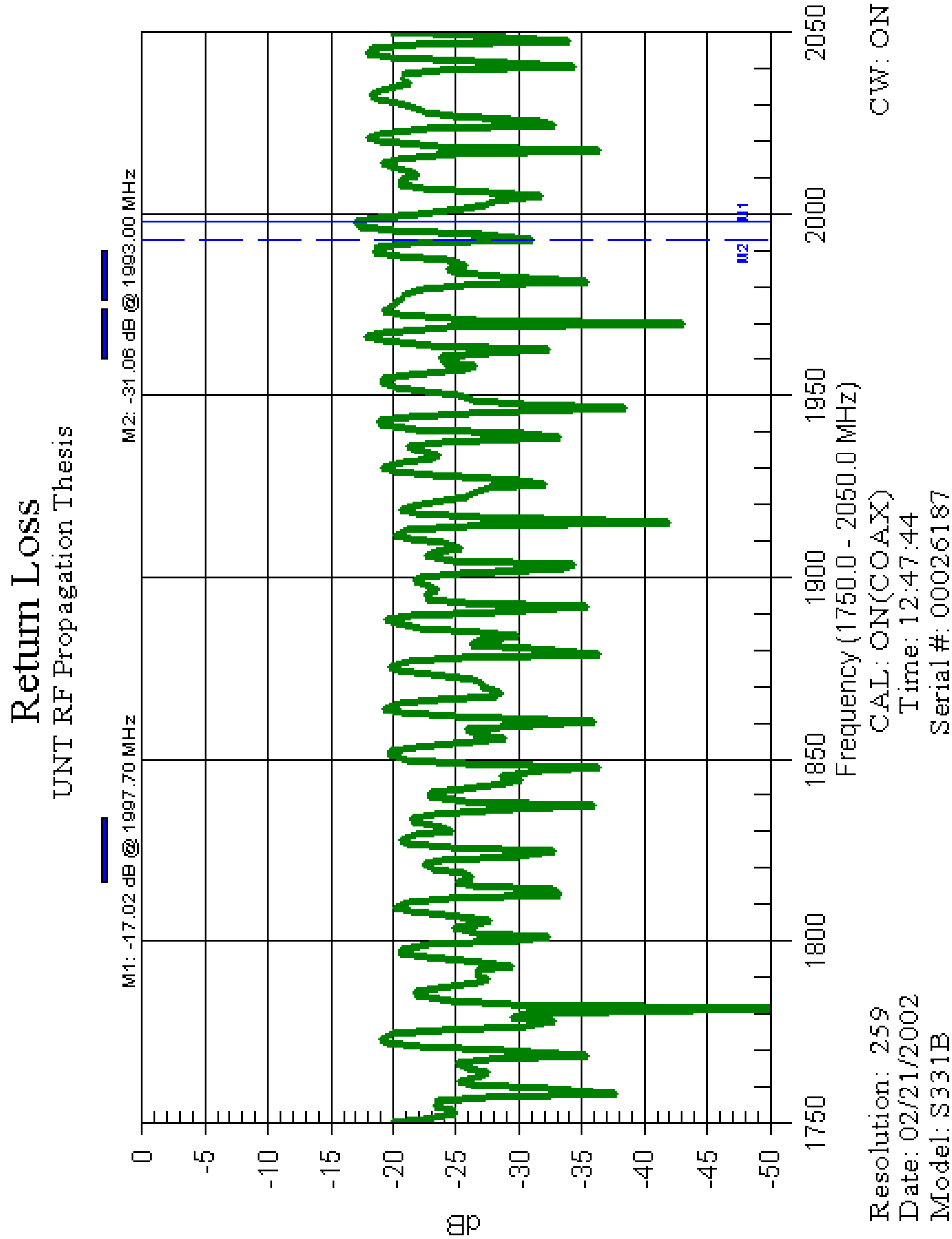
Return Loss
UNT RF Propagation Thesis
M1: -17.02 dB @ 1997.70 MHz
M2: -31.06 dB @ 1993.00 MHz
dB
0
-5
-10
-15
-20
-25
-30
-35
-40
-45
-50
1750
1800
1850
1900
1950
2000
2050
M1
M2
Frequency (1750.0 - 2050.0 MHz)
Resolution: 259
Date: 02/21/2002
Model: S331B
CAL: ON(COAX)
Time: 12:47:44
Serial #: 00026187
CW: ON

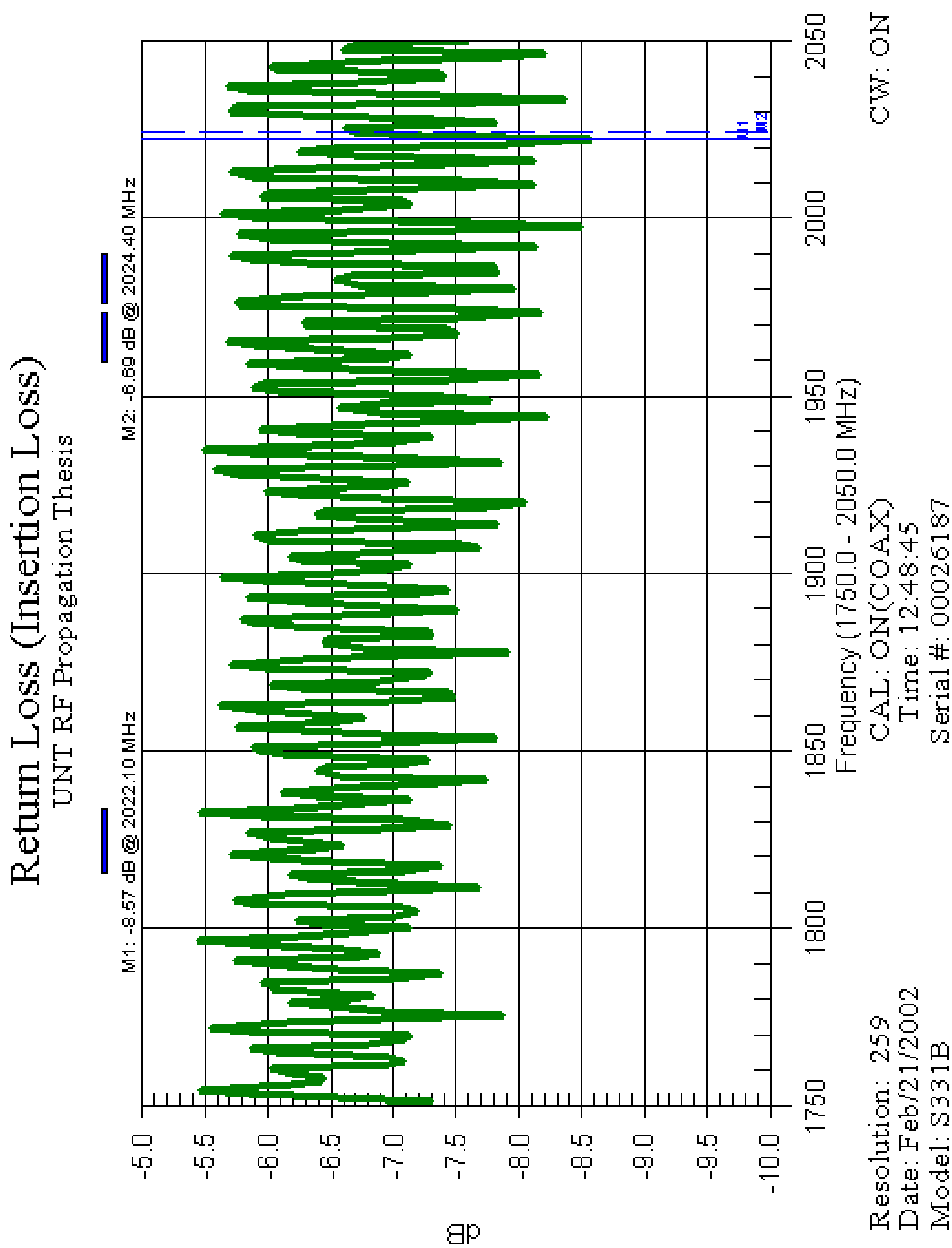
Return Loss (Insertion Loss)
UNT RF Propagation Thesis
M1: -8.57 dB @ 2022.10 MHz
M2: -6.69 dB @ 2024.40 MHz
dB
-5.0
-5.5
-6.0
-6.5
-7.0
-7.5
-8.0
-8.5
-9.0
-9.5
-10.0
1750
1800
1850
1900
1950
2000
2050
Frequency (1750.0 - 2050.0 MHz)
CAL: ON(COAX)
Time: 12:48:45
Serial #: 00026187
Resolution: 259
Date: Feb/21/2002
Model: S331B
CW: ON

APPENDIX I

ANTENNA TESTS GRAPHS

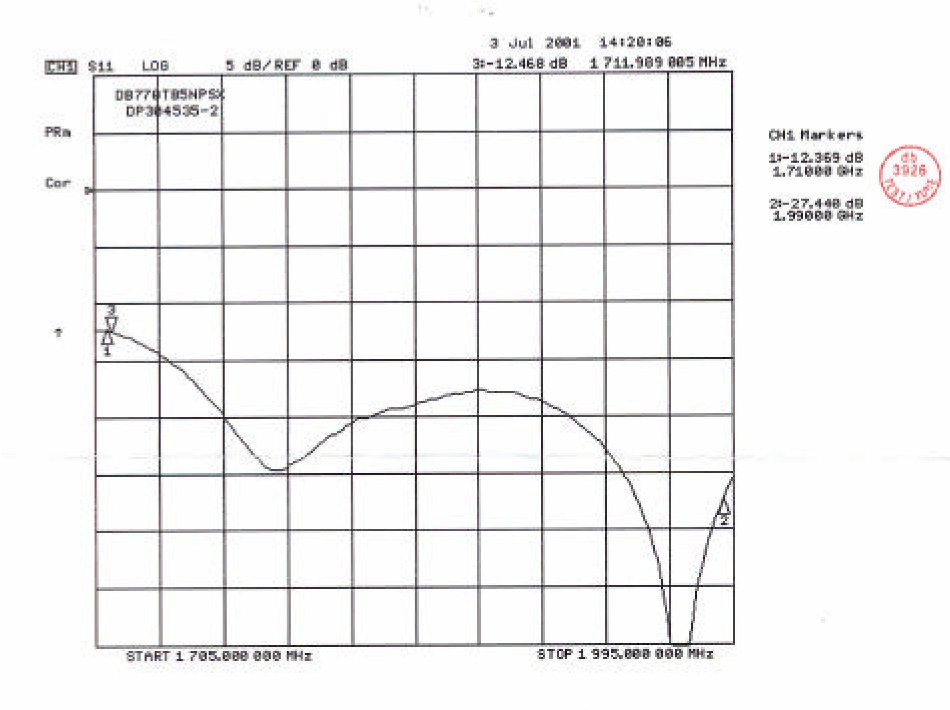
3 Jul 2001 14:20:06
CH1 S11 LOG 5 dB/ REF 0 dB 3:-12.468 dB 1 711.909 005 MHz
DB770TB5NPSX
DP304535-2
PRm
Cor
CH1 Markers
1:-12.369 dB
1.71000 GHz
2:-27.440 dB
1.99000 GHz
START 1 705.000 000 MHz
STOP 1 995.000 000 MHz

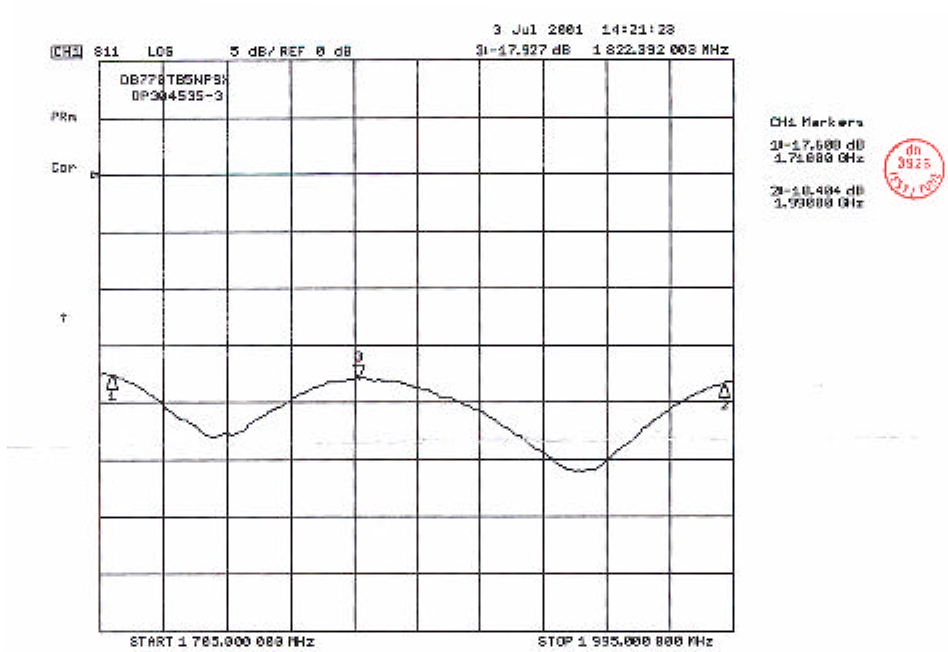
3 Jul 2001 14:21:23
CH1 S11 LOG 5 dB/ REF 0 dB 3:-17.927 dB 1 822.392 003 MHz
DB778TB5NPSX
DP304535-3
PRm
Cor
CH1 Markers
START 1 705.000 000 MHz
STOP 1 995.000 000 MHz

REFERENCES

[1] Agilent Technologies, Inc., *User's Guide: Agilent Technologies ESA Spectrum Analyzers.* Santa Rosa, CA, Agilent Technologies, Inc., 2000.

[2] Agilent Technologies, Inc., *Calibration Guide: Agilent Technologies ESA Spectrum Analyzers.* Santa Rosa, CA, Agilent Technologies, Inc., 2000.

[3] Agilent Technologies, Inc., *Specifications Guide: Agilent Technologies ESA Spectrum Analyzers.* Santa Rosa, CA, Agilent Technologies, Inc., 2000.

[4] Agilent Technologies, Inc., *Programmer's Guide: Agilent Technologies ESA Spectrum Analyzers.* Santa Rosa, CA, Agilent Technologies, Inc., 2001.

[5] Andrew Corporation, *Catalog 38.* Orland Park, IL, Andrew Corporation, 2001.

[6] Anritsu Company. "Site Master™ Cable and Antenna Analyzer [25 MHz to 4000 MHz]" [web site online]. Richardson, TX, Anritsu Company, 2000 [cited 14 August 2002]. Available from http://www.us.anritsu.com/products/showProducts.aspx/prod.97; INTERNET.

[7] Astrolab, Inc. "Power Handling of RF Coaxial Cable Assemblies." [web site online]. Warren, NJ, Astrolab, Inc., 2001 [cited 16 April 2002]. Available from

http://www.rf.rfglobalnet.com/library/ApplicationNotes/files/2/astrolab.app.txt.htm; INTERNET.

[8] Bertoni, H. L., *Radio Propagation for Modern Wireless Systems.* Upper Saddle River, NJ, Prentice-Hall, Inc., 2000.

[9] Bishop, R. H., *LabVIEW Student Edition 6i.* Upper Saddle River, NJ, Prentice-Hall, Inc. 2001.

[10] Blaunstein, N., *Radio Propagation in Cellular Networks.* Norwood, MA, Artech House, Inc., 2000.

[11] Consumer Information Bureau. "Market Sense: Cellphones; Facts, Fiction and Frequency." Washington, DC: Federal Communications Commission, 2000.

[12] Decibel Products "DB770TB5NPXS 6 dBd Triple Band Indoor Antenna" [web site online]. Dallas, TX, Allen Telecom Company., 2001 [cited 29 January 2002]. Available from http://www.decibelproducts.com/ProductNotebookAntenna2.asp?Param=ModelNumber&Model=DB770TB5NPXS&freq=on; INTERNET.

[13] Dersch, U., and Zollinger, E., "Propagation Mechanism in Microcell and Indoor Environments," *IEEE Trans on Vehicular Technology,* Vol. 43, No.4, pp1058-1066, Nov. 1994.

[14] Devore, J. L., *Probability & Statistics for Engineering and the Sciences: Second Edition.* Belmont, CA, Brooks/Cole Publishing Company, 1987.

[15] Dodd, A.Z., *The Essential Guide to Telecommunications: Second Edition.* Upper Saddle River, NJ, Prentice-Hall, Inc., 2000.

[16] The Dow Chemical Company. "Styrofoam Brand Insulation – Technical Center." [web site online]. Midland, MI, The Dow Chemical Company, 2001 [cited 2 October 2001]. Available from http://www.dow.com/styrofoam/na/dowpro/arch/comm/tecctr/index.htm; INTERNET.

[17] Durgin, G.D. "Advanced Site-Specific Propagation Prediction Techniques." Master's Thesis, Virginia Polytechnic Institute and State University, 1998.

[18] Eastpoint Technologies, LLC "Refractive Index." [web site online]. Manchester, NH, Eastpoint Technologies, LLC., 2001 [cited 5 October 2001]. Available from http://www.plasticsusa.com/refract.html; INTERNET.

[19] Enduro Systems, Inc. "Tuff Span Fiberglass Panel Products." [web site online]. Houston, TX, Enduro Systems, Inc., 2000 [cited 2 October 2001]. Available from http://www.endurocomposites.com/prime/html/products/tuffspan/tuffspan_main.htm; INTERNET.

[20] Ertel, R.B. "Antenna Array Systems: Propagation and Performance." PhD Dissertation, Virginia Polytechnic Institute and State University, 1999.

[21] GE Plastics. "GE Plastics – LEXAN 101." [web site online]. Pittsfield, MA, General Electric Company, 2001 [cited 2 October 2001]. Available from http://www.geplastics.com/resins/datasheets/americas/lexan/101.html; INTERNET.

[22] Gibson, J.D., *The Mobile Communications Handbook*. Boca Raton, FL, CRC Press, Inc., 1996.

[23] Hewlett-Packard Company, *Operation and Service Guide: 8648A/B/C/D Signal Generator*. Santa Rosa, CA, Hewlett-Packard Company, 1999.

[24] Holloway, C. L. and Perini, P. L., "Analysis of Composite Walls and Their Effects on Short-Path Propagation Modeling," *IEEE Trans on Vehicular Technology*, Vol. 46, No.3, pp730-738, Aug. 1997.

[25] Honcharenko, W. and Bertoni, H. L., “Transmission and reflection characteristics at concrete block walls in the UHF bands proposal for future PCS,” *IEEE Trans on Antennas and Propagation*, Vol. 42, No.2, pp232-239, Feb. 1994.

[26] HUBER+SUHNER AG. “Technical Data of N50 Connectors.” [web site online]. Herisau, Switzerland, HUBER+SUHNER AG, 2000 [cited 29 January 2002]. Available from http://www.hubersuhner.com/p-rf/p-rf-con/p-rf-con-overview/p-rf-con-n50/p-rf-con-n50-td.htm ; INTERNET.

[27] Kim, S., Guarino, Jr., B. J., Willis III, T. M., Erceg, V., Fortune, S. J., Valenzuela, R. A., Thomas, L. W., Ling, J., and Moore, J. D., “Radio Propagation Measurements and Prediction Using Three-Dimensional Ray Tracing in Urban Environments at 908 MHz and 1.9 GHz,” *IEEE Trans on Vehicular Technology*, Vol. 48, No. 3, May 1999.

[28] Lindgren RF Enclosures, Inc. “DEI Shielding Materials” [web site online]. Glendale Heights, IL, Lindgren RF Enclosures, Inc., 2001 [cited 29 January 2002]. Available from http://www.lindgrenrf.com/index2.htm ; INTERNET.

[29] Local and State Government Advisory Committee, “A Local Government Official’s Guide to Transmitting Antenna RF Emission Safety: Rules, Procedures, and Practical Guidance.” Washington, DC: Federal Communications Commission, 2000.

[30] Loctite. "Polystyrene PS" [web site online]. Rocky Hill, CT, Loctite, 2000 [cited 4 October 2001]. Available from http://www.loctite.com/literature_html/pdf/pgs62-63.pdf; INTERNET.

[31] Massey, S. E. "Church Bell Tower conceals Cellular Telephone Site." [web site online]. York, PA, Buchart-Horn, Inc., 1997 [cited 14 November 2000]. Available from http://www.bh-ba.com/97fa_4.html; INTERNET.

[32] National Instruments Corporation, "NI LabVIEW" [web site online]. Austin, TX, National Instruments Corporation, 2002 [cited 14 August 2002]. Available from http://sine.ni.com/apps/we/nioc.vp?cid=1381&lang=US; INTERNET.

[33] Ohio State University, ElectroScience Laboratory, "Test Summary: PCS on floor (VP) 1700MHz-1950MHz" [web site online]. Columbus, OH, Stealth Network Technologies, Inc., 1998 [cited 15 November 2000]. Available from http://esl.eng.ohio-state.edu/abstracts/abstracts.html; INTERNET.

[34] Pacific Cellsite Systems Inc. "Services." [web site online]. Irvine, CA, Pacific Cellsite Systems Inc., 1999 [cited 13 October 2000]. Available from http://www.paccellsite.com/services/; INTERNET.

[35] Pegasus Technologies. "Indoor Radio Propagation." [web site online]. Lenoir City, TN, Pegasus Technologies, 2001 [cited 16 April 2002]. Available from http://www.sss-mag.com/indoor.html; INTERNET.

[36] Saunders, S.R., *Antennas and Propagation for Wireless Communication Systems.* New York, NY, John Wiley & Sons, Inc., 1999.

[37] Stealth Network Technologies, Inc. "Structural and RF Testing." [web site online]. North Charleston, SC, Stealth Network Technologies, Inc., 2000 [cited 13 October 2000]. Available from http://www.stealthsite.com/page.cfm?category=structural/RF%20Testing&product_id=45; INTERNET.

[38] Tabbane, S., *Handbook of Mobile Radio Networks.* Norwood, MA, Artech House, Inc., 2000.

[39] Tarng, J. H., Chang, W. R., and Hsu, B. J., "Three-dimensional Modeling of 900-MHz and 2.44-GHz Radio Propagation in Corridors," *IEEE Trans on Vehicular Technology*, Vol. 46, No.2, pp519-526, May 1997.

[40] TeleStructures, Inc. "Wireless Site Solutions for the Environmentally Conscious Community." [web site online]. Atlanta, GA, TeleStructures, Inc., 2000 [cited 13

October 2000]. Available from http://www.telestructures.com/home.htm; INTERNET.

[41] Tipler, P. A., *Physics: Second Edition.* New York, NY, Worth Publishers, Inc., 1982

[42] Tomasi, W., *Electronic Communications Systems: Fundamentals Through Advanced, Fourth Edition.* Upper Saddle River, NJ, Prentice-Hall, Inc., 2001.

[43] Valenzuela, R. A., Landron, O., and Jacobs, D. L., "Estimating Local Mean Signal Strength of Indoor Multipath Propagation," *IEEE Trans on Vehicular Technology,* Vol. 46, No.1, pp203-212, Feb. 1997.

[44] Wireless Telecommunications Bureau. "Broadband PCS Fact Sheet." [web site online]. Washington, DC, Federal Communications Commission, 2002 [cited 16 April 2002]. Available from http://www.fcc.gov/pcs/bbfctsh.html/; INTERNET.

[45] Wireless Telecommunications Bureau, "Fact Sheet: New National Wireless Tower Siting Policies." Washington, DC: Federal Communications Commission, 1996.

[46] Wireless Telecommunications Bureau, "Fact Sheet #2: New National Wireless Tower Siting Policies." Washington, DC: Federal Communications Commission, 1996.

[47] Wireless Telecommunications Bureau. "Wireless Facilities Siting Issues." [web site online]. Washington, DC, Federal Communications Commission, 2000 [cited 16 November 2000]. Available from http://www.fcc.gov/wtb/siting/; INTERNET.